Cluster structure of 8p-4h states in ^{20}Ne

M. M. Hindi,* J. H. Thomas, D. C. Radford,† and P. D. Parker
Wright Nuclear Structure Laboratory, Yale University, New Haven, Connecticut 06511
(Received 23 November 1981)

The structure of high-lying states in ^{20}Ne has been studied using the ^{12}C(^{12}C, α)^{20}Ne reaction at $E(^{12}\text{C}) = 64$ and 80 MeV. The spins and branching ratios to the $\alpha + ^{16}$O channel were determined by measuring double (α-α) and triple (α-α-γ) angular correlations. The branching ratios for decay to the ^{12}C + ^{8}Be channel were obtained from an α-^{12}C coincidence experiment. In addition to confirming the spins of several lower-lying states, we have made a spin assignment of 8^+ for the state at 18.538 MeV and also suggest assignments to states at 17.259 MeV (7^-), 20.478 MeV (8^+), and 24.378 MeV (7^-). The 13.927-MeV (6^+) state is assigned to the $K^\pi = 0_2^+$ band, and it is suggested that this band also includes the 8^+ state at 20.478 MeV. The 18.538-MeV (8^+) state was found to have a large reduced width for decay into ^{12}C + ^{8}Be which, together with its small reduced width for decay to $\alpha + ^{16}\text{O}_{\text{g.s.}}$, suggests that it has a large ^{12}C + ^{8}Be cluster parentage. This state appears to be the 8^+ member of a new 8p-4h band which has the 12.436-MeV (0_6^+) state as its band head and the state at 15.159 MeV as its 6^+ member. The discovery of such a rotational band in ^{20}Ne with a large ^{12}C + ^{8}Be cluster parentage and a large moment of inertia provides the first direct indication of correlations between the α clusters in 8p-4h states.

[NUCLEAR STRUCTURE ^{20}Ne; measured spins, parities, branches to $\alpha + ^{16}$O and ^{12}C + ^{8}Be; deduced reduced widths, cluster structure.]

I. INTRODUCTION

Light nuclei exhibit a wide variety of phenomena from independent particle motion, to collective rotational and vibrational features, to clustering characteristics. The many-body nature of the nuclear physics problem, even in these light nuclei, has necessitated the use of different models, each of which describes one particular aspect of the data. Models in which the nucleus is divided into an alpha cluster plus core have been successful in reproducing the large α-particle widths and large spectroscopic factors for α transfer, as well as the rotational features and enhanced $E2$ transitions which are observed between particular states in these light nuclei.[1] Prompted by this success, attempts have been made recently to extend these models to include more complicated cluster configurations.[1] By generalizing these models and enlarging the cluster model space, the overlap with the shell model should increase, and more aspects of the data should be reproduced. Therefore, it is important to establish the existence of states with new cluster configurations and to investigate their properties in order to furnish a testing ground for these new cluster calculations. In this paper, we report on an investigation of states in ^{20}Ne which have a cluster structure other than the well-known $\alpha + ^{16}$O configuration.

The nucleus ^{20}Ne is probably one of the most extensively studied light nuclei; it has been studied using shell model,[2] Hartree-Fock,[3] and cluster model calculations.[1] The $\alpha + ^{16}$O cluster structure of the $K^\pi = 0^-$ and $K^\pi = 0_4^+$ rotational bands has been well established experimentally[4,5] and cluster model calculations based on the $\alpha + ^{16}$O cluster structure[1,6] have been able to reproduce these two bands, as well as the ground state band, all of which have four particles outside an ^{16}O core as their dominant shell model configuration. The $\alpha + ^{16}$O cluster model space is not large enough, however, to reproduce the well-known rotational bands[7] built on the 6.72 MeV (0_2^+), 7.191 MeV (0_3^+), and the 4.968 MeV (2^-) states, and there have been several attempts to reproduce these bands by including more complicated cluster configurations in the model space.[1,8,9]

The only cluster calculation which has been at all successful in this regard is the coupled-channel-orthogonality-condition–model (CCOCM) calculation of Fujiwara *et al.*,[9] who use $\alpha + ^{16}$O cluster states coupled to ^{12}C + ^{8}Be cluster states. In particular, by including the ^{12}C + ^{8}Be cluster structure they reproduce, for the first time in a cluster calcu-

lation, the band built on the 7.191 MeV (0_3^+) state. Experimentally, members of this band are found to have very small α reduced widths[7] and very weak proton strengths,[10] but they are strongly populated in ^{8}Be transfer reactions and hence are thought to have an eight particle four hole (8p-4h) configuration.[11] The 2^+, 4^+, and 6^+ members of the $K^\pi=0_3^+$ band have all been well established; however, there has been no definite confirmation of the 8^+ or higher spin members. Therefore, it was the aim of this study to search for high spin members of this $K^\pi=0_3^+$ band as well as any high-lying 8p-4h states and to determine whether any of those states has a predominantly $^{12}C+{}^8Be$ cluster structure. To that end we have measured the spins, parities, and branching ratios for decay to the $\alpha+{}^{16}O$ and $^{12}C_{g.s.}+{}^8Be_{g.s.}$ channels of several high-lying states in ^{20}Ne. Our results suggest the existence of a new 8p-4h band in ^{20}Ne with a large $^{12}C+{}^8Be$ cluster structure.

To populate high spin states of possible 8p-4h character, we chose the $^{12}C(^{12}C,\alpha)^{20}Ne$ reaction for two reasons. First, the low spin members of the $K^\pi=0_3^+$(8p-4h) band are found to be strongly excited in this reaction.[11-13] Second, the spinless nature of the beam, target, and ejectile makes it possible to determine the spin of the residual nucleus from angular correlation measurements. Previous studies on the $^{12}C(^{12}C,\alpha)^{20}Ne$ reaction were limited to bombarding energies $E(^{12}C)\leq 72$ MeV,[7] and most of this work was done below 63 MeV. At the lower bombarding energies the reaction is found to have a predominantly compound nature, except for the population of the low spin members of the $K^\pi=0_3^+$ band, where a considerable direct component is found.[13] To investigate the selectivity of the reaction at higher bombarding energies, where states of high spin and excitation are expected to be strongly populated because of the larger angular momentum and energy brought in by the beam, we measured α particle spectra at $\theta_\alpha\approx 0°$ in steps of 1 or 2 MeV over the bombarding energy range $60\leq E(^{12}C)\leq 80$ MeV. It was found that at these bombarding energies the reaction is reasonably selective and relatively direct, in the sense that a relatively small number of states are populated with roughly the same relative strength over this wide range of bombarding energies. There are over 150 levels known in ^{20}Ne below $E_x=21$ MeV,[7] and therefore the consistent population of relatively small number of levels over this range of bombarding energies suggests that they might have a special, perhaps 8p-4h, character.

All of these measurements were conducted using the Yale MP-1 Tandem Van de Graaff accelerator facility; the experimental techniques and details of our measurements will be discussed in Sec. II; for a more detailed description of the experimental equipment and procedures used in these measurements, see Ref. 14. In Sec. III we will present the spins and branching ratios extracted from the reduced data and compare our results to those obtained recently by other authors. In Sec. IV the character of the observed states and their assignment to rotational bands will be discussed, with particular emphasis on those having a $^{12}C+{}^8Be$ cluster structure.

II. EXPERIMENTAL PROCEDURES

A. Spin measurements

To determine the spins of states in ^{20}Ne we measured

$$^{12}C(^{12}C,\alpha_0)^{20}Ne(\alpha_1)^{16}O\ ,$$

α_0-α_1, double angular correlations in the Litherland-Ferguson method II geometry[15] at $E(^{12}C)=80$ MeV for those ^{20}Ne states which decay to the $J^\pi=0^+$ ground state of ^{16}O. For those ^{20}Ne states which decay to excited states in ^{16}O with spin $J\neq 0$, triple angular correlation measurements (e.g., Fifield *et al.*[16]) were used. In this technique the angular distribution of the alpha particles from the decay $^{20}Ne^*(J_A)\rightarrow\alpha_1+{}^{16}O^*(J_B)$ is made sensitive to the spin J_A by detecting the gamma ray from the decay

$$^{16}O^*(J_B)\rightarrow{}^{16}O_{g.s.}+\gamma$$

at a fixed angle in coincidence with α_0 and α_1 (see Fig. 1). The triple angular correlation expression and its properties are described in detail in Refs. 14, 16, and 17, and will not be repeated here.

The triple angular correlation experiment could not be carried out at $E(^{12}C)=80$ MeV, because of the sensitivity of the NaI($T1$) detectors to the prolific number of background γ rays and neutrons produced at that energy. Reducing the beam energy re-

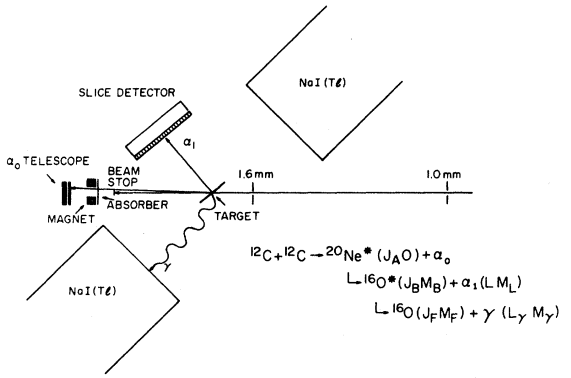

FIG. 1. Schematic diagram of the experimental setup used in the α_0-α_1-γ triple correlation experiment.

sulted in substantially smaller γ-ray and neutron counting rates and made the experiment feasible. A beam energy of 64 MeV was chosen because the α_0 singles spectrum at this energy closely resembled that at 80 MeV, and therefore comparisons could be made between the results extracted at these two energies.

A schematic diagram of the instrumentation used in the α-α-γ, triple angular correlation experiment is shown in Fig. 1. The states in ^{20}Ne were populated using the ^{12}C(^{12}C,α)^{20}Ne reaction at $E(^{12}\text{C})=64$ MeV. The target was a self-supporting carbon foil 100 μg/cm^2 thick, with its normal tilted 45° from the beam direction. The primary ^{12}C beam was stopped by a water-cooled circular piece of tantulum (3 mm in diameter, 1.6 mm thick and supported by a 1 mm wide vertical strip) located 7 cm from the target. The forward scattered ^{12}C ions were stopped in a stack of fifteen 2 mg/cm^2 Havar foils.

The primary alpha particle (α_0) was detected in a ΔE-E telescope consisting of two 50 mm^2 Si(SB) detectors. The telescope was centered at 0° behind a 6.35 mm diameter collimator placed at 10 cm from the target; the aperture subtended a geometrical solid angle of 3.17 m sr, but the useful solid angle of the detector telescope was restricted to 1.82 m sr by the beam stop; the angle of detection was $0.6° \lesssim \theta_{\alpha_0} \lesssim 2.3°$.

The alpha particles (α_1) from the decay of states in ^{20}Ne were detected in a 16-slice position-sensitive detector (PSD) similar to the one described in Ref. 16. The length of the detector (50 mm) spanned 50.6° in the laboratory system ($35° \lesssim \theta_{\text{lab}} \lesssim 85°$), corresponding to $55° \lesssim \theta_{\alpha_1}$ (r.c.m.) $\lesssim 130°$ in the ^{20}Ne recoiling center of mass system (r.c.m.); in the laboratory frame, the solid angle subtended by each slice varied from 11.3 m sr for the end slices to 18.0 m sr for the middle ones, and the corresponding angular width varied from 2.5° to 3.6°. The angles at the center of each slice were measured to better than ±0.1°.

Gamma rays from the decay of ^{16}O* were detected in two 7.62 cm×7.62 cm NaI(Tl) crystals placed 8 cm from the target at an angle of $(\theta,\Phi)=(45°,180°)$ and [since the triple angular correlation is symmetric under the transformation $(\theta,\Phi)\rightarrow(\pi-\theta,\pi+\Phi)$] at an angle of (135°,0°) to augment the count rate (Fig. 1).

Standard NIM electronic instrumentation was used to process and analyze the various pulses from each of the detectors and to define the following six types of events: (1) α_0-α_1-γ triple coincidence, (2) α_0-α_1 double coincidence, (3) α_0-γ double coincidence, (4) α_0 singles, (5) α_1 singles, and (6) γ singles. The double coincidence events α_0-α_1 and α_0-γ were defined by fast coincidences between α_0 and α_1 ($\Delta t_{\text{FWHM}} \lesssim 10$ nsec) and α_0 and γ ($\Delta t_{\text{FWHM}} \approx 2$ nsec) (where FWHM is full width at half maximum), respectively. A triple coincidence event (α_0-α_1-γ) was defined by a slow time coincidence ($\Delta t_{\text{resolving}} \lesssim 2$ μsec) between a fast α_0-α_1 coincidence and a fast α_0-γ coincidence: the seven analog signals (ΔE_{α_0}, E_{α_0}, P_{α_1}, E_{α_1}, E_γ, $\text{TAC}_{\alpha_0\text{-}\alpha_1}$,$\text{TAC}_{\alpha_0\text{-}\gamma}$) were fed into analog-to-digital converters (ADC's) interfaced with the laboratory's IBM 360/44 computer. The data acquisition system was programmed to recognize the six events mentioned above and to transfer the contents of the associated ADC's directly to the computer memory for monitoring and for on-line analysis. The coincidence and α_0 singles events were analyzed on-line and were also written on magnetic tape, event-by-event, for later off-line reanalysis.

The α_0-α_1 double coincidence events were analyzed to generate the α_1 angular distribution for decays to (a) the ground state of ^{16}O, (b) the doublet at 6 MeV, and (c) the doublet at 7 MeV. The α_0-α_1-γ triple coincidence events were analyzed to generate the α_1 angular distribution for decays to (a) the 6.13 MeV (3^-) state in ^{16}O and (b) the doublet at 7 MeV. The decay channel was identified kinematically from a two-dimensional plot of E_{α_1} versus E_{α_0} at each α_1 angle (as defined by the slices of the α_1 detector). An example of such a plot is shown in Fig. 2. To separate out decays to $^{16}\text{O}_{\text{g.s.}}$, it was sufficient to draw software gates on the 2-d plot with a light pen attached to the display system. In order to make the separation between decays to the 6-MeV

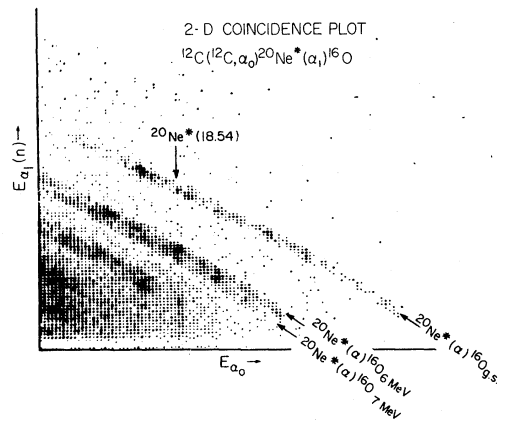

FIG. 2. Two-dimensional plot of the energy of the decay alpha particle (α_1) which is detected in slice n of the position sensitive detector versus the α_0-particle energy.

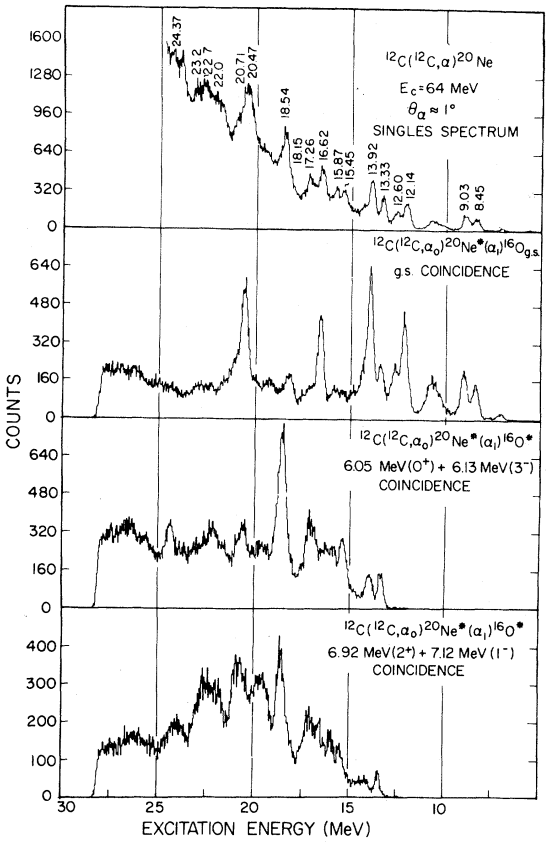

FIG. 3. Comparison of the singles spectrum for the reaction ^{12}C(^{12}C,α)^{20}Ne with double (α_0-α_1) coincidence spectra in which the ^{20}Ne* states α decay to various final states in ^{16}O.

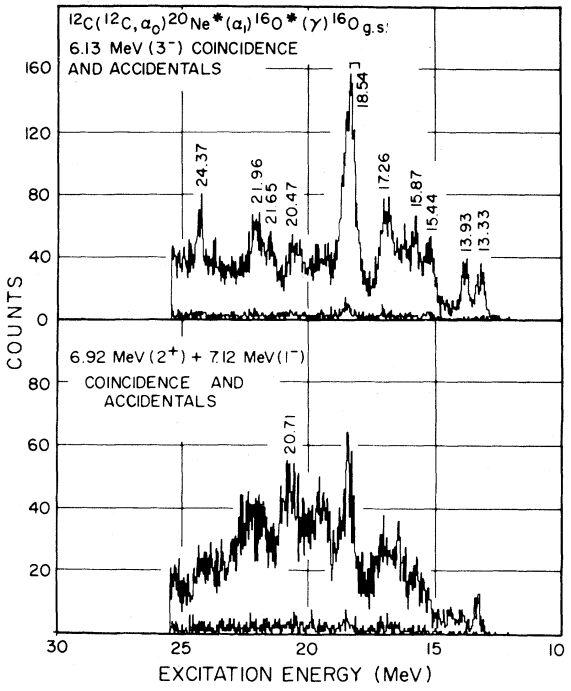

FIG. 4. Triple (α_0-α_1-γ) coincidence spectra for the decay of ^{20}Ne* states to excited states in ^{16}O. Also shown to the same scale are the accidentals spectra.

doublet and those to the 7-MeV doublet, it was necessary to generate more accurate gates (for each angle) from an analysis of full-resolution (1024-channels) E_{α_1} spectra. The triple coincidence spectra were generated by requiring (in addition to the requirements met by the α_0-α_1 double coincidence events) a true time coincidence between the α_0 particle and a γ ray with $E_\gamma > 700$ keV. The latter requirement eliminated events corresponding to the decay

$$^{20}\text{Ne}^* \rightarrow \alpha + {}^{16}\text{O}(6.05, 0^+) ,$$

since the 6.05 MeV (0$^+$) state decays only by e^+e^- pair emission. Both doubles and triples accidentals spectra were also generated, and both were found to be negligible.

Plotted as a function of excitation energy in ^{20}Ne, Fig. 3 shows a sample of the E_{α_0} singles spectrum as well as the sum over all angles of the double coincidence spectra for the decay of ^{20}Ne* to (1) the ground state of ^{16}O, (2) the doublet at 6 MeV, and (3) the doublet at 7 MeV. Triple coincidence spectra for decays to the 6.13 MeV (3$^-$) state and to the 7 MeV doublet are shown in Fig. 4. The resemblance between the triple coincidence spectrum for decay to ^{16}O(6.13) and the double coincidence spectrum for decay to ^{16}O(6.05 + 6.13) (Fig. 3) indicates that none of the states populated by this reaction in this region of excitation in ^{20}Ne has a predominant decay to the 6.05 MeV (0$^+$) state.

The angular correlation yields for the decay of each state of interest in ^{20}Ne to the various final states in ^{16}O were extracted from the double and triple coincidence data using multi-Gaussian fits to the E_{α_0} coincidence spectra. The resulting yields were converted to yields in the ^{20}Ne r.c.m. system, thus putting them in a form suitable for comparison with the theoretical angular correlations. The data and the procedure followed in determining the spins from them will be presented in Sec. III.

Singles and coincidence spectra for the 80 MeV run are shown in Fig. 5. Although these spectra are quite similar to those obtained at 64 MeV (Fig. 3), some differences do exist, and these will be discussed in Sec. III B.

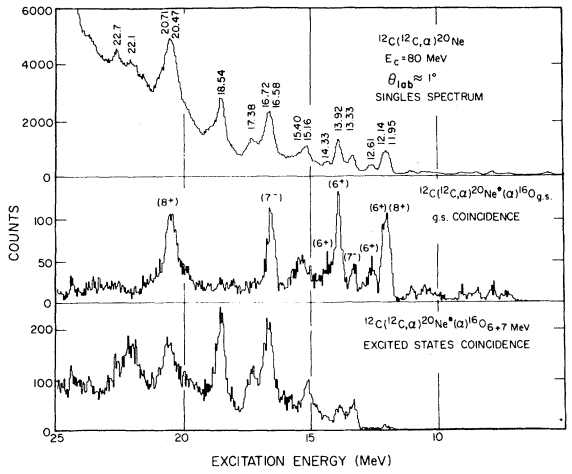

FIG. 5. Comparison of the singles and double coincidence spectra obtained during the double correlation experiment at $E(^{12}C)=80$ MeV.

B. $^{12}C + {}^{8}Be$ branching ratio measurement

To measure the branching ratio for the decay $^{20}Ne^* \rightarrow {}^{12}C + {}^{8}Be$, we performed[18] an α-^{12}C double coincidence measurement of the

$$^{12}C(^{12}C,\alpha)^{20}Ne^*(^{12}C)^{8}Be$$

reaction at $E(^{12}C)=80$ MeV. The α particles were detected at 0° in a telescope identical to the one described above for the $(\alpha$-$\alpha)$ and $(\alpha$-α-$\gamma)$ angular correlation measurements. The ^{12}C's were detected in two ΔE-E telescopes, one placed at 15 cm from the target and at $\theta_{lab}=20°$, and the other at 10 cm and rotated to collect data at 24° and 28° ($51° \lesssim \theta_{r.c.m} \lesssim 83°$). The ΔE detectors were

$$10\ \mu m \times 25\ mm^2\ Si(SB)\ ,$$

and the E detectors were

$$50\ \mu m \times 50\ mm^2\ Si(SB)\ .$$

Both telescopes had 4.95 mm diameter collimators, thus subtending 0.86 m sr and 1.93 m sr for the far and near telescopes, respectively. The α particles and the ^{12}C's were detected in fast time coincidence with $\Delta t_{FWHM} \approx 16$–$18$ nsec, which gave a real-to-random ratio of 5:1 for the forward detector telescope and 9:1 for the backward one.

In addition to the identification of the α's and the ^{12}C's through their respective telescopes, the kinematic correlation between their energies was used to identify the three body final state

$$^{12}C + {}^{12}C \rightarrow \alpha + {}^{12}C_{g.s.} + {}^{8}Be_{g.s.}\ .$$

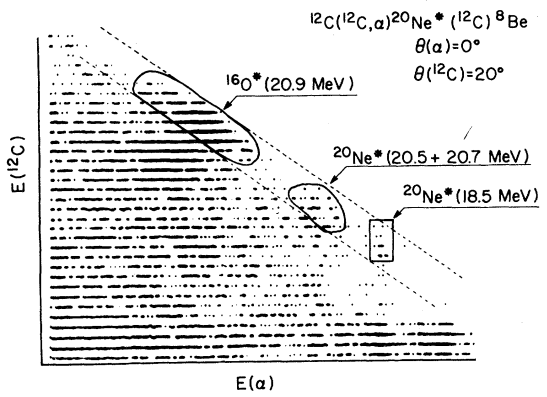

FIG. 6. Two-dimensional plot of the ^{12}C energy versus the α-particle energy for α-^{12}C double coincidence events. (Channels with ≤ 1 count are blanked out.) Events corresponding to the three-body final state ($^{12}C + {}^{8}Be + \alpha$) lie along the boundary of the four-body ($^{12}C + \alpha + \alpha + \alpha$) phase space. The dashed lines enclose the region corresponding to this boundary; this region was projected onto the $E(\alpha)$ axis to generate the spectra in Fig. 7. Peaks in this region correspond to final state interactions between the components of the three-body final state; these final state interactions are labeled in this spectrum and are enclosed by solid lines (to guide the eye).

A two dimensional plot of $E(\alpha)$ versus $E(^{12}C)$ is shown in Fig. 6. A software gate was drawn around the region corresponding to the $\alpha + {}^{12}C_{g.s.} + {}^{8}Be_{g.s.}$ three body final state, with a width in the E_C direction corresponding approximately to the energy spread in E_C due to $\Delta\theta$; counts inside this gate were projected onto the E_α axis. The resulting coincidence spectra, with accidentals ($\lesssim 1$ count/channel) subtracted, are compared to the singles spectrum in Fig. 7. The peaks at 18.5 MeV and at 20.5 + 20.7 MeV show up at essentially the same position at all angles and clearly correspond to the sequential decay through $^{20}Ne^*$,

$$^{12}C + {}^{12}C \rightarrow {}^{20}Ne^* + \alpha(0°)$$
$$\searrow\ {}^{12}C_{g.s.}(\theta) + {}^{8}Be_{g.s.}$$

rather than through $^{16}O^*$. The strongest peak in these coincidence spectra does show a substantial change in position with the ^{12}C detector angle and corresponds to the sequential decay through $^{16}O^*$,

$$^{12}C + {}^{12}C \rightarrow {}^{16}O^* + {}^{8}Be_{g.s.}$$
$$\searrow\ \alpha(0°) + {}^{12}C_{g.s.}(\theta)$$

involving the 20.9 MeV (7^-) state in ^{16}O.

The singles and coincidence yields were extracted

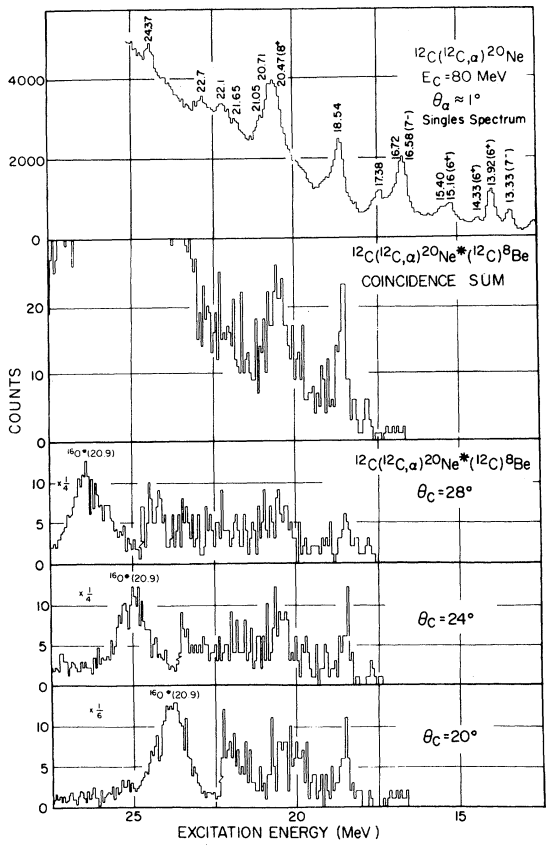

FIG. 7. Comparison of the singles spectrum for the reaction ^{12}C(^{12}C,α)^{20}Ne, with the coincidence spectra in which the ^{20}Ne* states decay to ^{12}C$_{g.s.}$ + ^{8}Be$_{g.s.}$ with the coincident ^{12}C detected at θ_{lab}=20°, 24°, and 28°.

from these spectra using Gaussian fits. The branching ratios extracted from these yields are presented in Sec. III A.

C. High resolution measurements

The use of thick targets (which was necessitated by the low count rate of coincidence events) and the requirement of protecting the 0° telescope with absorber foils resulted in an energy resolution which was too poor to resolve close-lying states and to extract their widths and excitation energies accurately. In order to obtain more precise excitation energies and widths for the ^{20}Ne states being populated in our experiments, we made high resolution measurements of these same ^{12}C(^{12}C,α)^{20}Ne spectra in singles experiments conducted with thin targets and with no absorbers at E(^{12}C)=48, 64, and 80 MeV. The beam was collimated using two rectangular apertures (width=1 mm and height =4.5 mm) placed at 50 cm and 127 cm from a 10 μg/cm^2 ^{12}C

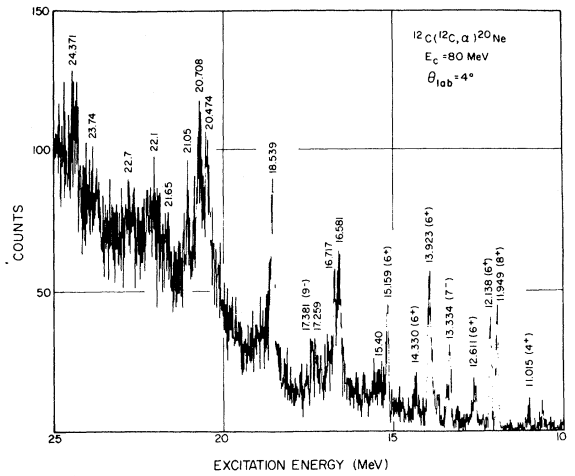

FIG. 8. High resolution spectrum of the ^{12}C(^{12}C,α)^{20}Ne reaction at E(^{12}C)=80 MeV, plotted as a function of excitation energy in ^{20}Ne.

target (normal to the beam). The α particles were detected at 4° in a ΔE-E telescope placed behind a 3-mm×6-mm collimator located 36 cm from the target. The measured instrumental resolution was 97±2.5 keV as determined from the measured widths of peaks corresponding to well-known narrow states. An accurate calibration of the spectra was obtained by using the excitation energies of well-known low-lying states in an intercomparison of the peak positions in these three spectra. The 80 MeV and 64 MeV high-resolution spectra are shown in Figs. 8 and 9, respectively. The excitation energies and widths of the populated states were extracted from the spectra by fitting the peaks with multi-Gaussian fits superimposed on a quadratic background and by unfolding the contribution of the

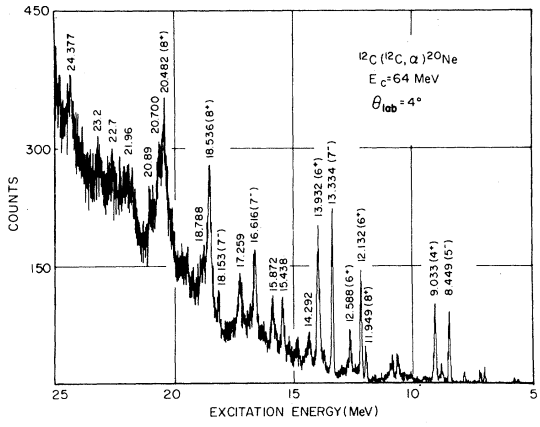

FIG. 9. High resolution spectrum of the ^{12}C(^{12}C,α)^{20}Ne reaction at E(^{12}C)=64 MeV, plotted as a function of excitation energy in ^{20}Ne.

TABLE I. Summary of excitation energies, widths, spins, and decay branching ratios of levels observed in the present study.

E_x (MeV±keV)		$\Gamma_{c.m.}$ (keV)		J^π				Decay branching ratios						
Previous results[a]	Present results	Previous results[a]	Present results	Previous results[a]	Present results $(\alpha-\alpha_0)_{80}$	$(\alpha-\alpha_0)_{64}$	$(\alpha\text{-}\alpha\text{-}\gamma)_{64}$[e]	α_0[c] (%)	α_0 (%)	α_{1+2}[c] (%)	α_{1+2} (%)	α_{3+4}[c] (%)	α_{3+4} (%)	$^{12}C + {}^{8}Be$ (%)
8.4486± 2.3		0.013		5^-		5^-			89±10					
9.030 ± 5		3.2		4^+		4^+			110±10					
11.949 ± 5		0.035		8^+	8^+									
12.134 ±10	12.135± 5	0.13		6^+	6^+	6^+			90± 6					
12.591 ±10	12.600± 10	88	50± 10	6^+	6^+	6^+			70±20					
13.334 ± 6		0.08[b]		7^-		7^-		43±1[d]	40± 6	57±1[d]				
13.904 ±20	13.927± 5	100	113± 7	6^+	6^+	6^+			72± 6					
14.307 ±10	14.311± 15	<100	<50	6^+	6^+				90±20					
15.160 ±15	15.159± 5		60± 15	6^+				2±2		46±2		52±2		
15.336 ±15	15.40 ± 40	380	410±130	7^-	(7^-)			32±2	60±15	58±2		10±2		
	15.438± 10		100± 20						20± 5		57± 7		23± 4	
15.879 ±15	15.872± 10	<250	100± 15	8^+[c]				9±2	24± 5	79±2	51± 7	12±4	25± 5	
16.577 ±12[f]	16.600± 15	86±6[f]	160± 30	7^-	7^-	7^-		72±3	60±10	20±3	20± 5	8±3	20± 5	
16.709 ±14[g]	16.717± 10	14±7[g]	37± 10	(3^-)[g]				5±2	$\lesssim$19	52±2		43±2		
	17.259± 11		162± 20				$7^-(9^-)$		15± 2		50± 6		35± 7	
18.06	18.153± 10			7^-[c]				71±6		29±6		<7		
	18.538± 7		138± 13				8^+		1.8±0.9		60± 8		26± 4	12±1.2
	20.478± 11		250± 30		(8^+)				66±26		14± 7			13±2.5
20.67	20.704± 11		~120	9^-[c]				61±3	$\lesssim$14	24±2	25±15	15±2	46±22	5±1
	20.89 ± 30													
	21.05 ± 20		140± 50											
	21.65 ±100		240± 50				$(7^-,9^-)$							
	22.03± 70		630± 80				(8^+)							
	22.7 ± 70		490±110											
	23.2 ±100		300±100											
	24.74±100		230±100											
	23.374±30		210± 50				$7^-(5^-)$							

[a]Reference 7.
[b]Reference 41.
[c]References 17 and 20.
[d]Reference 16.
[e]J^π values extracted from triple correlation assuming $L = L_{min}$.
[f]Reference 24.
[g]References 24 and 25.

TABLE II. Comparison of the excitation energies and widths extracted from our high-resolution measurements at $E(^{12}C)=64$ and 80 MeV.

E_x (MeV±keV)			$\Gamma_{c.m.}$ (keV)		
$E_c=80$ MeV	64 MeV	Average	80 MeV	64 MeV	Average
12.138± 5	12.132± 5	12.135± 5			
12.611± 10	12.588± 5	12.600±10	130± 20	50± 10	
13.923± 5	13.932± 5	13.927± 5	121± 10	105± 10	113± 7
14.330± 10	14.292± 10	14.311±15	<50	100± 20	
15.159± 5			60 ± 15		
15.40 ± 40			410±130		
	15.438± 10			100± 20	
	15.872± 10			100± 15	
16.581± 10	16.616± 10	16.600±15	150± 30	173± 20	160± 30
16.717± 10			37 ± 10		
17.259± 15	17.259± 15	17.259±11		162± 20	
	18.153± 10				
18.539± 10	18.536± 10	18.538± 7	125± 25	143± 15	138± 13
20.474± 15	20.482± 15	20.478±11	220± 50	270± 40	250± 30
20.708± 15	20.700± 15	20.704±11		~120	
	20.89 ± 30				
21.05 ± 20			140± 50		
21.65 ± 100			240± 50		
22.1 ± 100	21.96 ±100	22.03 ±70	550±100	800±150	630± 80
22.7 ± 100	22.7 ±100	22.7 ±70	500±150	480±150	490±110
	23.2 ±100		300±100		
23.74 ± 100			230±100		
24.371± 40	24.377± 40	24.374±30	200± 50	270±130	210± 50

instrumental resolution in quadrature. Based on interlocking comparisons of known states observed in the high resolution spectra measured under identical conditions and gain settings at $E(^{12}C)=48$ and 64 MeV and at $E(^{12}C)=64$ and 80 MeV, direct comparisons can be made between the measured alpha-particle energy for the highly excited states of interest and for well-known states ~10 MeV lower in excitation. The results are given in Table I. A comparison between the results extracted from the 64-MeV data and from the 80-MeV data is shown in Table II.

III. EXPERIMENTAL RESULTS AND ANALYSES

A. Extraction of spins and branching ratios

1. Spins

The measured double and triple angular correlations were fitted with the appropriate theoretical correlation expressions. For the α-α-γ measurements described here (see Fig. 1) [$\theta_{\alpha_0}=0°$; $J_F=0$ and $L_\gamma=L_{\gamma'}=J_B$], the theoretical correlation has the form[16]

$$W_{\rm th}(\theta_{\alpha_1},\Phi_{\alpha_1},\theta_\gamma,\Phi_\gamma)=\sum_{M_B,M_B',L,L'}\langle J_BM_BL-M_B\,|\,J_A0\rangle\langle J_BM_B'L'-M_B'\,|\,J_A0\rangle$$
$$\times\langle||L||\rangle\langle||L'||\rangle^*Y_L^{-M_B}(\theta_{\alpha_1},\Phi_{\alpha_1})Y_{L'}^{*-M_B'}(\theta_{\alpha_1},\Phi_{\alpha_1})$$
$$\times\sum_{k,q}(-1)^{J_B-M_B'}\left[\frac{4\pi}{2k+1}\right]^{1/2}Q_kR_k(J_BJ_BJ_B0)\langle J_BM_BJ_B-M_B'\,|\,kq\rangle Y_k^q(\theta_\gamma,\Phi_\gamma)\,,$$

where the R_k's are the angular distribution coefficients of Rose and Brink,[19] the Q_k's are attenuation coefficients[14] which take account of the finite solid angle of the γ-ray detector and the effects of the hyperfine interaction and the finite lifetime of the $^{16}O^*$ state, and the quantities $\langle||L||\rangle$ are the reduced matrix elements for the decay $^{20}Ne^*\rightarrow{}^{16}O^*+\alpha$, with L restricted by the conservation of angular momen-

tum and parity.

For the α_0-α_1 measurements described here [$\theta_{\alpha_0}=0°$; $J_B=0$ and $L=J_A$ and $M_A=M_B=M_L=0$] the theoretical correlation reduces to the form

$$W_{\text{th}}(\theta_{\alpha_1},\Phi_{\alpha_1})=\frac{2J_A+1}{4\pi}\,|P_{J_A}(\cos\theta_{\alpha_1})|^2 .$$

An isotropic background term was also included as a free parameter in the fit in order to take account of the continuous background present in the coincidence spectra (Figs. 3, 4, and 5). This background corresponds to real coincidences from the decay of broad low spin states in ^{20}Ne, from direct three body breakup, and from the kinematic inversion of the primary and decay alpha particles [$\alpha_1\rightarrow 0°$ and $\alpha_0\rightarrow\theta$]. Although Young[20] has demonstrated that in some cases such background can have considerable angular structure, the use of an isotropic background is empirically justified in the present case by the fact that the yields at the minima in the angular correlations are nearly constant, and by the fact that, in the present data, in those cases where the spins are already well established, the correlation function [$W_{\text{th}}(\Omega_i)+C$] gives a good fit to the data. In all of the cases for which we have made definite spin assignments, the background extracted from the fit was consistent with the background-to-peak ratio in the sum of the coincidence spectra, and was, in general, fairly small.

In the case of the double correlations there are only two free parameters in the fit, the background term C and a multiplicative factor normalizing W_{th} to the data. For the α-α-γ triple angular correlations, the L involved in the decay

$$^{20}\text{Ne}(J_A)\rightarrow{}^{16}\text{O}(J_B)+\alpha_1(L)$$

can take the values

$$L_{\min}=|J_A-J_B|,(L_{\min}+2),\ldots,(J_A+J_B) ,$$

and hence each of the reduced matrix elements $\langle||L||\rangle$ can be taken as a free parameter. However, since the angular momentum barrier strongly favors decay via the lowest allowed L value, and since the triple correlation is insensitive[16] to small admixtures of the next lowest allowed L, $(L_{\min}+2)$, initial fits to the data were made for different J_A values with L restricted to $L_{\min}$; here again, therefore, there are only two free parameters, C and $\langle||L_{\min}||\rangle$, which serve as a normalization parameter. These initial fits usually eliminated all but one or two J_A values. Improvements to these fits were then sought by allowing both $\langle||L_{\min}||\rangle$ and $\langle||L_{\min}+2||\rangle$ to vary. If asymmetries in the experimental correlation were evident, or if two different J_A's both seemed to reproduce the structure of the experimental correlation, then improvements to these fits were sought by generalizing the angular correlation expression to take account of the possible interference of each of these states with the background or with intrinsically overlapping states of different spin. The phases for the two different J_A's were set equal to either 0° (complete coherent interference) or 90° (complete incoherent interference). Although the fitting program could fit the generalized reduced matrix elements $\langle||J_A,L||\rangle$ for all the allowed L values for two interfering J_A's, with the phases allowed to vary, to have allowed the phases and all the allowed L values to vary simultaneously would have increased the number of free parameters to the point where any spin assignment based on such fits would have had very little credibility. All assignments which we have made are for those cases in which the data and the analysis are both clear enough to allow the correlation fits to be made using only two [C and $\langle||J_A,L_{\min}||\rangle$] or three [$C$,$\langle||J_A,L_{\min}||\rangle$, and $\langle||J_A,L_{\min}+2||\rangle$] or [$C$,$\langle||J_A,L_{\min}||\rangle$, and $\langle||J'_A,L_{\min}||\rangle$] free parameters. The experimental correlations and the resulting fits and spin assignments for each individual state are presented in Sec. III B.

2. *Branching ratios*

The branching ratios for the decay of the ^{20}Ne states to the $^{12}C_{g.s}+{}^{8}Be_{g.s.}$ channel and to the

$$\alpha+{}^{16}\text{O(g.s.; } 6.05+6.13;\ 6.92+7.12)$$

channels were obtained from a comparison between the ^{12}C(^{12}C,α)^{20}Ne singles counts and the coincidence counts for the

$$^{12}\text{C}(^{12}\text{C},\alpha)^{20}\text{Ne}(^{12}\text{C})^{8}\text{Be}$$

and the

$$^{12}\text{C}(^{12}\text{C},\alpha)^{20}\text{Ne}(\alpha)^{16}\text{O}$$

experiments together with a knowledge of the solid angles and angular correlation involved. Because of kinematic broadening it was not possible to separate the $\alpha+{}^{16}$O (6.05 MeV) and $\alpha+{}^{16}$O (6.13 MeV) decay channels, or to separate the $\alpha+{}^{16}$O (6.92 MeV) and $\alpha+{}^{16}$O (7.12 MeV) decay channels on the basis of the α_1 spectra. A separation of these channels based on the analysis of the coincident γ-ray spectra was also not possible because of the poor energy resolution in the γ-ray spectra resulting from the very high counting rate in the NaI(Tl) detectors. Coincidence losses due to the high count rate in the slice detector were corrected on the basis of the measured count rate loss of a pulser fed through the slice detector preamplifier. The extracted branching

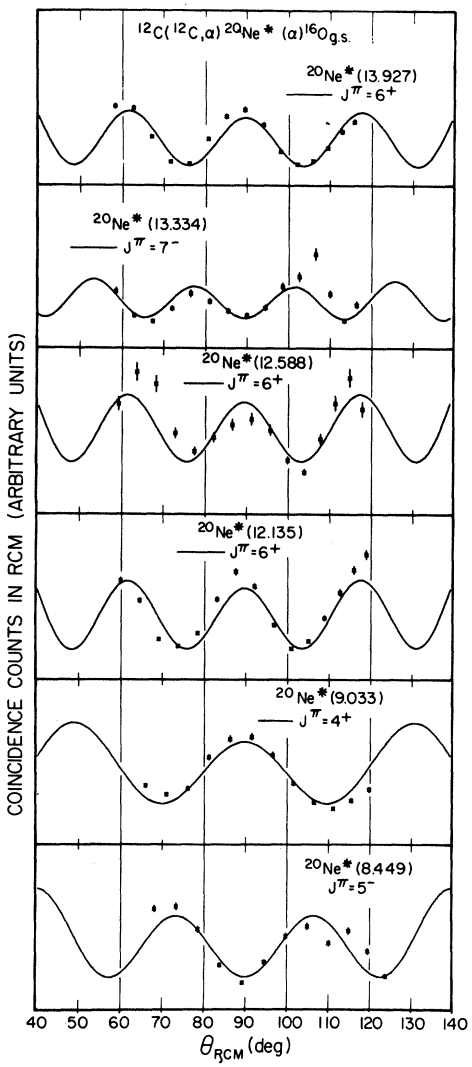

FIG. 10. Double angular correlations for the decay of the 8.449-MeV, 9.033-MeV, 12.135-MeV, 12.558-MeV, 13.334-MeV, and 13.927-MeV states in ^{20}Ne to ^{16}O$_{g.s.}$. The curves are fits using a $|P_J|^2$ + const angular dependence. The data were taken at $E(^{12}C)=64$ MeV.

ratios for the decay of each state to various channels are given in Table I.

B. Results for individual states

1. States with $E_x < 14$ MeV

Figure 10 shows the double angular correlations and the resulting spin assignments for the states at 8.45 MeV (5^-), 9.03 MeV (4^+), 12.14 MeV (6^+), 12.60 MeV (6^+), 13.33 MeV (7^-), and 13.93 MeV (6^+). These correlations confirm the known spin assignments for these states.[7] [The level which we observe in the 80 MeV high resolution spectrum (Fig. 8) at 12.611±0.01 MeV ($\Gamma=130\pm20$ keV), whose spin we have determined to be 6^+ from the double correlation experiment at 80 MeV, and whose g.s. branching ratio is 82±25%, is most likely the same as the 12.588-MeV level observed at $E(^{12}C)=64$ MeV; the higher excitation energy and larger width extracted in the 80-MeV spectrum are probably due to a weakly populated level unresolved from the tail on the high-excitation-energy side of the 12.611-MeV peak in the 80-MeV high resolution spectrum (Fig. 8).]

The agreement between our results for states below 14 MeV and the previously determined assignments for several well-known states verifies our experimental procedures and supports the credibility of our assignments to states at higher excitation.

2. States with $14 < E_x < 16$ MeV

Mehta *et al.*[21] assign a spin of 6^+ to a broad ($\Gamma=240$ keV) level at 14.3 MeV; Young *et al.*[20] also observed a broad ($\Gamma=240$ keV) level at 14.26 MeV in their

$$^{12}C(^{12}C,\alpha)^{20}Ne(\alpha)^{16}O$$

studies, but they were unable to extract a definite spin for the state even though the correlation seems to have a $|P_6|^2$ structure. Young *et al.*,[20] therefore, raised the possibility that the broad peak which they observed was a doublet although correlations for separate halves of the peak were quite similar. Artemov *et al.*[22] also observed a peak at 14.3±0.1 MeV in their

$$^{16}O(^6Li,d)^{20}Ne^*(\alpha)^{16}O$$

studies for which they measured a width of ≈100 keV and suggested a spin of 6^+.

In our studies a level at $E_\alpha=14.330\pm0.01$ MeV with $\Gamma<50$ keV is populated at $E(^{12}C)=80$ MeV (Figs. 8 and 5), and the angular correlation for the decay of this level to $^{16}O+\alpha_0$ (Fig. 11) suggests a spin of 6^+ for this level. The state at $E_\alpha=14.292\pm0.01$ MeV which is populated weakly at $E(^{12}C)=64$ MeV (Fig. 9) is quite possibly the same state, but it was too weak to be resolved from the 13.93-MeV state in our 64-MeV coincidence data (Fig. 3), and therefore its spin was not measured in our correlations. If these were instead two separate levels, then our data would support the hypothesis of Young *et al.*, for two narrow levels at 14.3 MeV at least one of which seems to have a spin of 6^+.

The broad level at $E_x=15.40$ MeV that we see in the 80 MeV spectrum (Fig. 8) decays predominantly to the ground state of ^{16}O (Fig. 5). Although its measured α-α correlation (Fig. 11) is not clear

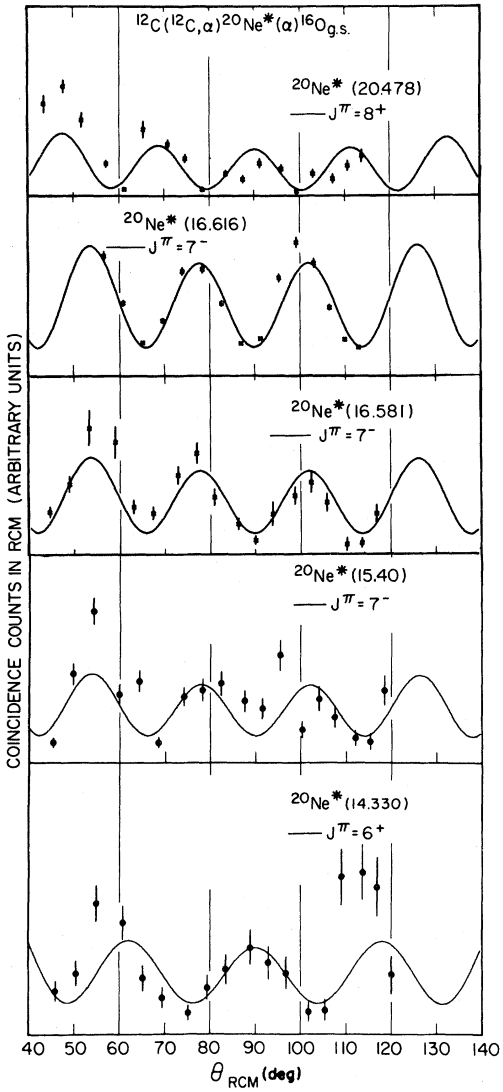

FIG. 11. Double angular correlations for the decay of the states in ^{20}Ne at 14.330, 15.40, 16.581, 16.616, and 20.478 MeV to $^{16}O_{g.s.}$. The curves are fits using a $|P_J|^2$ + const angular dependence. The data for the states at 14.330, 15.40, 16.581, and 20.478 MeV were measured at $E(^{12}C)=80$ MeV; the data for the state at 16.616 MeV were measured at $E(^{12}C)=64$ MeV.

enough to allow a definite spin assignment to be made, the angular correlation suggests a spin of 7^-, which supports the identification of this level with the well-known 7^- state at 15.336 ± 0.015 MeV ($\Gamma=380\pm60$ keV).[7] Our measured g.s. branching ratio for this state ($60\pm15\%$) is somewhat smaller than the $90\pm10\%$ reported by Sanders *et al.*[5] and by Artemov *et al.*[22] Panagioutou *et al.*[12] observe a level at 15.4 MeV in the $^{12}C(^{12}C,\alpha)^{20}Ne$ reaction at $E(^{12}C)=45$ MeV, for which they report branching ratios of 70% to $^{16}O_{g.s.}$, 15% to $^{16}O(6.05+6.13)$, and 15% to $^{16}O(6.92+7.12)$. They make no spin assignment for this level but suggest an identification with the 7^- level. Young *et al.*[20] observed a broad structure at 15.36 MeV in the $^{12}C(^{12}C,\alpha)^{20}Ne$ reaction at $E(^{12}C)=56$ MeV. The branching ratios he extracts are 32% to $^{16}O_{g.s.}$, 58% to $^{16}O(6.05+6.13)$, and 10% to $^{16}O(6.92+7.12)$. The width and excitation energy of the peak appearing in his excited-states coincidence spectrum are slightly different from those of the peak appearing in the ground state coincidence spectrum, leading Young to suggest that more than one level is populated in this region of excitation at that bombarding energy. The possible existence of a narrow state unresolved from the 15.4 MeV level (which would explain the difference in branching ratios reported by the various groups) is supported by our 64 MeV data, where we see a relatively narrow ($\Gamma=100\pm20$ keV) level at 15.438 ± 0.10 MeV (Fig. 9), which decays predominantly to the excited states in ^{16}O. The triple angular correlation for the α-decay of this state to $^{16}O(6.13,3^-)$ is relatively structureless, and no spin assignment could be made.

3. *States with $16<E_x<17$ MeV*

In the high resolution spectrum measured at 80 MeV we observe one state[23] at $E_x=16.581$ MeV and one at $E_x=16.717$ MeV. These two states are not resolved in the 0° spectrum collected in the coincidence experiment (Fig. 5); however, from an analysis of the position and width of the 16.6-MeV peak in the ground-state and excited-states coincidence spectra, we conclude that the 16.581-MeV state decays predominantly ($\gtrsim46\%$) to the ground state of ^{16}O, while the 16.717-MeV state decays predominantly to the excited states at 6 and 7 MeV. The double angular correlation of the 16.581 MeV state for decay to $^{16}O_{g.s.}$ is shown in Fig. 11, together with the best fit, $J^{\pi}=7^-$.

The weak branching ratio of the 16.717 MeV state to $^{16}O_{g.s.}$ prevented the extraction of its spin from the g.s. angular correlation. If this state were also populated strongly at $E(^{12}C)=64$ MeV, then its spin could be measured in the triple angular correlation experiment; unfortunately, however, the high resolution spectrum at $E(^{12}C)=64$ MeV (Fig. 12) shows that only one state ($E_x=16.616$ MeV) is strongly populated in this region of excitation at $E(^{12}C)=64$ MeV. This state decays mainly to the ground state of ^{16}O, and the double angular correlation for this decay mode is shown in Fig. 11, together with the fit for $J^{\pi}=7^-$. The similarity in properties of this state and the state at 16.581 MeV observed at $E(^{12}C)=80$ MeV indicates that they are most likely the same state.

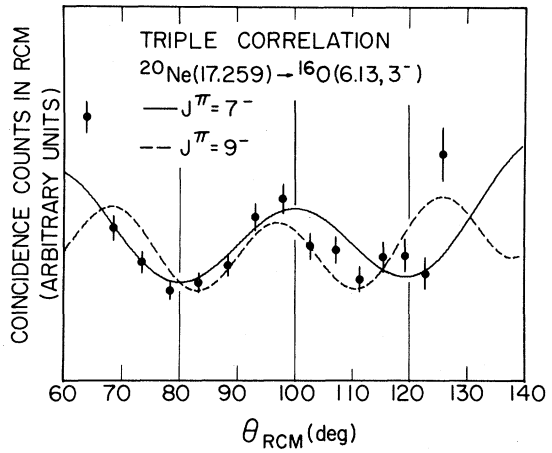

FIG. 12. Triple angular correlations for the decay of the 17.259-MeV level to ^{16}O(6.13-MeV, 3$^-$). The curves are the sum of a constant background plus the theoretical triple correlation for the decay of a state with spin J to a 3$^-$ state via $L=L_{\min}$. The data were taken at $E(^{12}C)=64$ MeV.

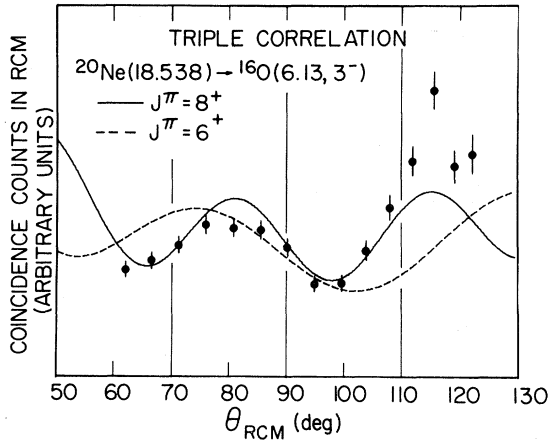

FIG. 13. Triple angular correlation for the decay of the 18.538-MeV state to ^{16}O (6.13-MeV, 3$^-$). The curves are theoretical triple correlations for the decay of a state with spin J^π via $L=L_{\min}$.

4. *The 17.26-MeV level*

In the 64-MeV high resolution spectrum (Fig. 9) we observe a level at $E_x=17.259$ MeV whose dominant decay mode is to the excited states of ^{16}O (Fig. 3 and Table I). The triple angular correlation for decay to the 6.13 MeV (3$^-$) state in ^{16}O is shown in Fig. 12, together with the best fits, which were for $J^\pi=7^-$ and 9$^-$; the fit with $J^\pi=7^-$, is slightly better ($\chi_\nu^2=3.9$ for the 7$^-$, and $\chi_\nu^2=6.6$ for the 9$^-$ fit). The predicted correlation for $J_A^\pi=8^+$ is out of phase with the data. The angular correlation for the decay to the 7-MeV doublet is featureless. Since a broad 8$^+$ level is known to exist at this excitation,[5,24,26] we attempted to fit the measured triple correlation for decay to the 6.13 MeV (3$^-$) state with a coherent admixture of 8$^+$ and 7$^-$ and with a coherent admixture of 9$^-$ and 8$^+$. In both cases the fitting procedure found only a very small admixture of the 8$^+$ component, and the χ_ν^2 did not improve at all.

It is clear that our level is not the well-known 9$^-$ level at 17.38±0.015 MeV which is a member of the $K^\pi=2^-$ band[7]; the width of that level is less than 10 keV, and its branching ratio to the ground state of ^{16}O is only ≈1% (Ref. 16); both of which are quite inconsistent with our results. It is also unlikely that the level measured in our triple correlation is the broad ($\Gamma\approx240$ keV) 9$^-$ level at 17.394 MeV (Ref. 24) since there is no evidence for our population of that state in our high-resolution spectrum (Fig. 9).

5. *The 18.54-MeV level*

The level at 18.538±0.007 MeV ($\Gamma=138\pm13$ keV) is strongly populated in our ^{12}C(^{12}C,α)^{20}Ne spectra at most bombarding energies between 64 and 80 MeV. There is good agreement in the excitation energies and widths extracted for this state in the analyses of the 64 MeV and 80 MeV high resolution data [$\Delta(E_x)\approx3$ keV and $\Delta(\Gamma)\approx18$ keV]; there is also good agreement between the decay branching ratios extracted for this state in the 64 and 80 MeV coincidence experiments. All of this evidence supports the idea that it is the same state which is being analyzed at both bombarding energies.

In the $\alpha_0+{}^{16}O_{g.s.}$ coincidence spectrum at 64 MeV (Fig. 3), the 18.54 MeV state appears only as a possible shoulder on the 18.15-MeV peak. Although the 18.15-MeV peak is not resolved from the 18.54-MeV peak in the low resolution singles spectrum [compared to the high resolution spectrum (Fig. 9) where the two peaks are well resolved], the centroid of the peak in the ground-state coincidence spectrum is shifted visibly to the right with respect to the centroids in the excited-states coincidence spectra, indicating that the 18.15-MeV state is the one decaying to the ground state of ^{16}O.

The triple angular correlation for the decay of the 18.54-MeV state to the 6.13-MeV (3$^-$) state in ^{16}O was fitted with the appropriate theoretical expression for various values of J_A assuming that the decay went through the lowest allowed L value. Figure 13 shows the experimental correlation, together with the fits for $J_A=8$ and $J_A=6$; the fit with $J_A=8$ is clearly superior to the fit with $J_A=6$. Figure 14 shows the resultant χ_ν^2 for the different J_A

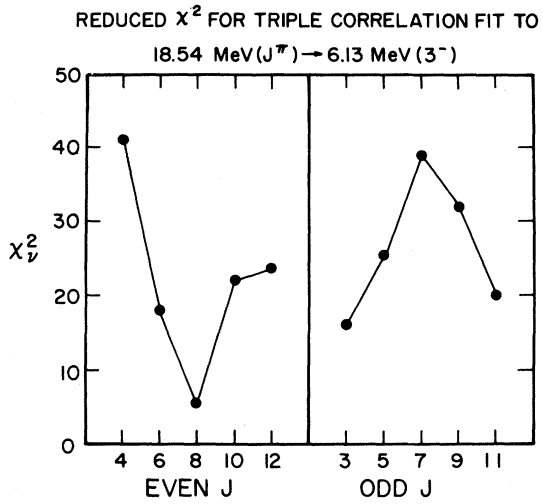

FIG. 14. Reduce χ^2 for triple correlation fits to the measured angular correlation for the decay ^{20}Ne* (18.54-MeV, J^π)$\rightarrow\alpha+{}^{16}$O (6.13-MeV, 3^-), plotted for various values of the spin J assuming the decay went through the lowest allowed L.

values. For even J_A the best fit was for $J_A=8$ and the next best fit was for $J_A=6$; correlations with odd J_A were completely out of phase with the data.

The $J_A=6$ correlation still could not fit the data when both $\langle L_{\min}\rangle$ and $\langle L_{\min}+2\rangle$ were allowed to vary freely. The value which was extracted from the data for

$$|\langle||L_{\min}+2||\rangle/\langle||L_{\min}||\rangle|^2$$

for $J_A=6$ was 2.0 ± 0.13, in contradiction to the ratio of the Coulomb penetrabilities

$$P_c\ (l=5)/P_c\ (l=3)=0.29\ .$$

In contrast, the ratio extracted for $J_A=8$ is 0.12 ± 0.03, which is in reasonable agreement with the value of

$$P_c\ (l=7)/P_c\ (l=5)=0.06\ .$$

6. *States with $20<E_x<21$ MeV*

In view of the fact that the 10^+ members of the $K^\pi=0_3^+$ (8p-4h) band is expected to be at $\approx$20.5 MeV, considerable effort was made in trying to establish uniquely the spins of the states at 20.478 ± 0.011 MeV ($\Gamma=250$ keV) and 20.704 ± 0.011 MeV ($\Gamma\sim120$ keV). Both of these states are populated at the bombarding energies of 80 and 64 MeV (Figs. 8 and 9). Although the two levels are not resolved in the coincidence spectra, the decay mode to the final states in ^{16}O can be determined from an analysis of the positions and widths of the peaks in

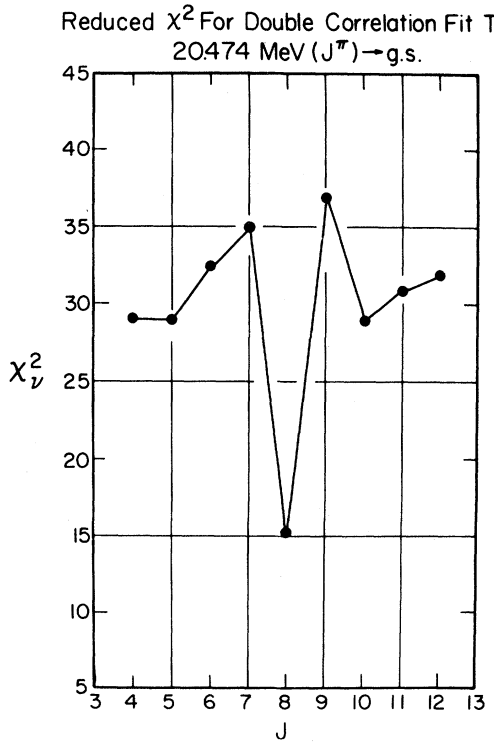

FIG. 15. Reduced χ^2 for double correlation fits to the measured double angular correlation for the decay of ^{20}Ne (20.474-MeV, J^π) to $^{16}O_{g.s.}$, plotted for various values of the spin J. The angular correlation was measured at $E(^{12}C)=80$ MeV.

the ground-state and excited-states coincidence spectra. The 20.7-MeV state decays mostly to the excited states in ^{16}O while the 20.5-MeV state decays mostly to the ground state of ^{16}O.

The double angular correlation for the ground-state decay of the 20.47 MeV state, measured at $E(^{12}C)=80$ MeV, is shown in Fig. 11, together with the best fit which is for $J^\pi=8^+$. Although the fit is not particularly good, no other J could reproduce the correlation, as can be seen from the plot of χ_ν^2 for various values of J (Fig. 15); the large χ_ν^2 for $J=7$ and 9 emphasize that this level has positive parity. A considerably improved fit is obtained if a small (10 to 15%) admixture of either $J^\pi=7^-$ or $J^\pi=6^+$ is allowed to interfere coherently with the $J^\pi=8^+$ correlation (Fig. 16). Although it is not clear which combination is best from these fits, it is clear that the dominant component is the $J^\pi=8^+$ one, and hence we tentatively assign a spin of 8^+ to the 20.474 MeV level.

The branching ratio for the decay of the 20.7-MeV state to the 6-MeV doublet is not very large, and the peak in the 6-MeV doublet coincidence spectra (Figs. 3 and 4) is dominated by the decay of the 20.5-MeV level. [The triple angular correlation for

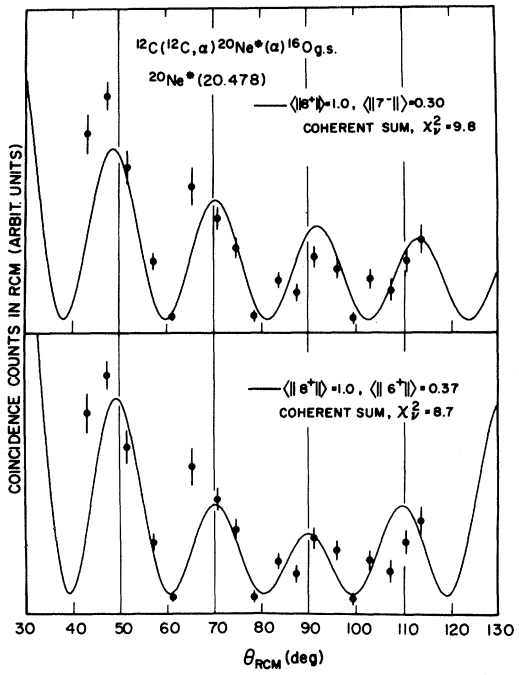

FIG. 16. Fits to the double angular correlation for the decay of the 20.478-MeV level in ^{20}Ne to $^{16}O_{g.s.}$ with a coherent admixture of 8^+ and 7^- (upper panel), and of 8^+ and 6^+ (lower panel). The fits have the angular dependence $(\langle||J||\rangle P_J + \langle||J'||\rangle P_{J'})^2 + \text{const}$. The data were taken at $E(^{12}C)=80$ MeV.

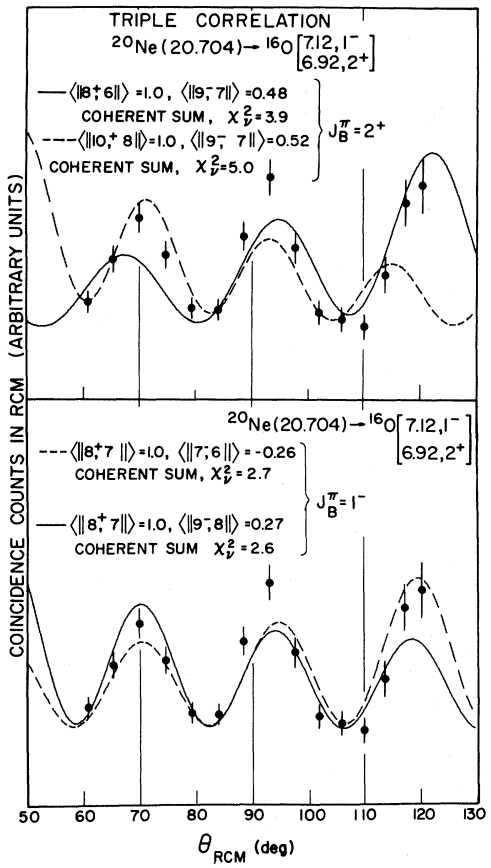

FIG. 17. Triple angular correlation for the decay of the 20.7-MeV peak in ^{20}Ne to ^{16}O (7-MeV). The curves in the upper panel are fits to the data with the theoretical triple correlation for the decay of a peak with the indicated coherent admixture of J^π values to a state with spin 2^+ via the lowest allowed L value; the curves in the lower panel are for decay to a state with spin 1^-.

the decay of the unresolved 20.5 + 20.7 MeV peak to the 6.13 MeV (3^-) state was extracted and, unsurprisingly, was found to be featureless.] The centroid of the unresolved (20.5 + 20.7)-MeV peak is shifted towards higher excitation energies in the coincidence spectra corresponding to decays to the (6.92 + 7.12)-MeV doublet (Figs. 3 and 4), indicating that most of those decays are coming from the 20.7- and 20.9-MeV states. However, the poor statistics in the triple coincidence data for these decays to the 7-MeV doublet prevented the extraction of yields for the separate 20.7- and 20.9-MeV components of the peak. Although the extracted triple correlation exhibits pronounced, regular structure (Fig. 17), it could not be fitted uniquely with the correlation of a single J_A decaying to $J_B=2^+$. The fits with $J_A=8$ and $J_A=10$ came closest to reproducing the structure of the data; however, both fits were unsatisfactory. Coherent admixtures of various other J_A values with $J_A=8$ and $J_A=10$ were also tried, and the best fits were those for 8 + 9 and 10 + 9 (Fig. 17). Both of these fits are very similar in quality, and a unique assignment of 8^+ or 10^+ to the structure centered at 20.7 MeV cannot be made, especially since the 9^- component in both fits is fairly large.

Substantially improved fits were obtained for this measured correlation under the assumption that the decay goes instead to the 7.12 MeV (1^-) state. In this case, there was a clear preference for $J_A=8^+$ (Fig. 17). Fits with $J_A=10^+$ plus coherent admixtures of various J_A's (still assuming $J_B=1$) failed to reproduce the data.

From the preceding considerations it is clear that although reasonable fits can be obtained for this measured correlation, there are substantial ambiguities concerning which state (or combination of states) in ^{20}Ne is decaying to which state (or combination of states) at 7 MeV in ^{16}O, so that no significant spin assignments can be made from this correlation at the present time.

The $^{16}O(\alpha,\alpha)$ scattering measurements[24,27] find a $J^\pi=9^-$ resonance at $E_x=20.683\pm0.009$ MeV ($\Gamma=75\pm9$ keV) with a branching ratio for decay to

$^{16}O_{g.s.}+\alpha$ of only $24.7\pm1.8\%$ which may not be inconsistent with our limit of $\lesssim 14\%$. (See footnote h, Table 20.21, Ref. 7, second entry.) Young's value[20] of 61% for this decay mode (assuming that the same state is involved) may come from an admixture of a contribution from the 20.5-MeV level whose dominant decay mode is the ground state of ^{16}O.

7. *States above $E_x = 21$ MeV*

Most of the peaks which we observed at $E_x > 21$ MeV were broad and seemed to consist of more than one level. In the coincidence experiments these peaks were not well enough resolved from background or from each other to enable the extraction of reliable yields for the determination of branching ratios; from a visual inspection of Figs. 3 and 5 we can see that these states decay mostly to the excited states in the $\alpha + {}^{16}O$ channel. In the triple coincidence spectrum for the decay to the 6.13-MeV (3^-) level (Fig. 4) distinct peaks at 21.65, 21.96, and 24.37 MeV were observed; the triple angular correlations were extracted and analyzed for each of these.

The triple angular correlation for the 21.65-MeV level was characteristic of spin 9^- or 7^-, while the correlation for the 21.96-MeV level could be fit with a coherent sum of $J_A = 8$ plus $J_A = 7$, with the 8^+ component being the dominant one. However, because of the poor quality of the fits and the poor statistics and the large background in the data, we cannot make definite spin assignments to either of these two levels.

The relatively narrow level at 24.37 MeV was observed at several bombarding energies above 64 MeV and is quite conspicuous at $E(^{12}C) = 76$ MeV. The excitation energies extracted for this level from the 64- and 80-MeV high-resolution spectra (Figs. 8 and 9) agreed to within $\lesssim 10$ keV, indicating that this peak does correspond to a well-defined level in ^{20}Ne. This is confirmed further by the fact that the peak in the coincidence spectra appears at the same α_0 energy for all α_1 angles. The relatively narrow width of this level at such a high excitation energy, where many decay channels are open, suggests that it has either high spin or a peculiar structure. The smoothly varying triple angular correlation measured for the decay of this state to the 6.13 MeV (3^-) state in ^{16}O is, however, characteristic of a spin of only 5^- or 7^-. Although the fits with $J_A = 7^-$ and $J_A = 5^-$ were equally poor, the fit for $J_A = 7^-$ was improved substantially upon allowing a coherent admixture of $J^\pi = 6^+$ (Fig. 18), while no coherent admixture was found which could equally improve the 5^- fit. Figure 18 also shows a fit with a coherent admixture of 5^- and 7^-. While a spin assignment of 7^- is preferred for this level, we cannot exclude the possibility of 5^-. The somewhat large admixture of the 6^+ component is probably due to interference with the fairly large background. We do not yet understand what the special configuration of this state could be that would allow it to be so narrow and selectively populated with a spin as low as 7^-.

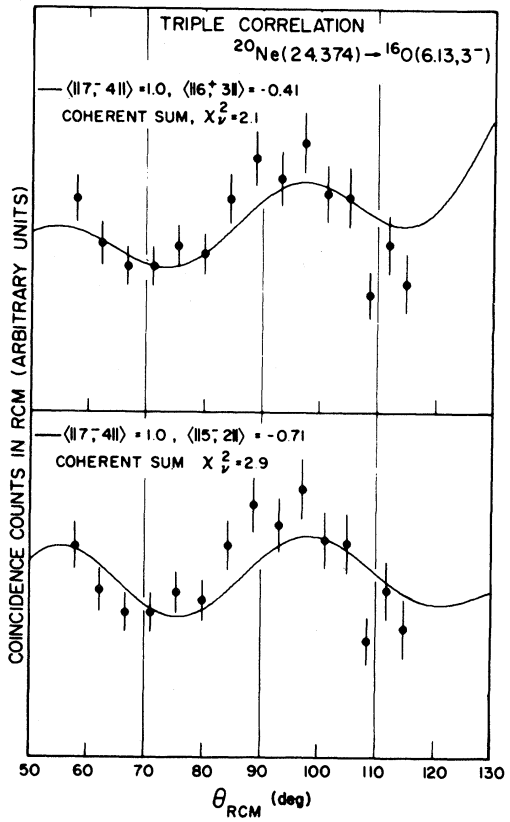

FIG. 18. Triple angular correlation for the decay of the 24.374-MeV state in ^{20}Ne to ^{16}O (6.13-MeV 3^-). The curves are fits using the sum of a constant background plus the theoretical triple correlation for the decay of a peak with a coherent admixture of $J^\pi = 7^-$ and 6^+ (upper panel) or $J^\pi = 7^-$ and 5^- (lower panel) to a 3^- state via the lowest allowed L.

IV. DISCUSSION

A. Reduced widths

The experimental arrangement of states into rotational bands is based on the comparison of the reduced widths for various electromagnetic and particle decay modes as well as on the usually linear relationship between E_x and $J(J+1)$. In particular, for the present study of the alpha-particle decays of states in ^{20}Ne, the reduced widths for states belonging to the same rotational band should be nearly the

TABLE III. Reduced widths of ^{20}Ne states observed in the present study. Branching ratios and total widths were taken from Table I, unless otherwise indicated. For the reduced width calculations, the following channel radii were used: $\theta_\alpha{}^2 \rightarrow R = 1.25(16^{1/3} + 4^{1/3}) = 5.134$ fm; $\theta_{^{12}C}{}^2 \rightarrow R = 1.4(12^{1/3} + 8^{1/3}) = 6.005$ fm.

E_x (MeV)	J^π	$\theta_{\alpha_0}{}^2$ (g.s.)	$\theta_{\alpha_2}{}^2$ (6.13)[e]	$\theta_{\alpha_3}{}^2$(6.92)[f]	$\theta_{^{12}C}{}^2$
8.4486	5^-	$(1.6 \pm 0.5)\times 10^{-3}$[a]			
9.030	4^+	0.022[a]			
11.949	8^+	$(7.6 \pm 2.2)\times 10^{-3}$[a]			
12.135	6^+	$(4.9 \pm 2.6)\times 10^{-4}$	0.66 ±0.36[b]		
12.600	6^+	0.09 ±0.02			
13.334	7^-	$(2.4 \pm 1.0)\times 10^{-4}$	0.025±0.010[d]		
13.927	6^+	0.10 ±0.01			
14.311	6^+	$\lesssim 0.45$			
15.159	6^+	$< 8\times 10^{-4}$	0.05 ±0.013	0.91±0.23	
15.872	8^+	0.047±0.013[c]	0.94 ±0.14[c]	4.2 ±0.9[c]	
16.600	7^-	0.10 ±0.02	0.048±0.013	0.44±0.12	
17.259	7^-	0.019±0.004	0.071±0.013	0.32±0.08	
	(9^-)	(0.25 ±0.05)	(0.92 ±0.17)	(13.4 ±3.3)	
18.538	8^+	$(3.2 \pm 1.5)\times 10^{-3}$	0.085±0.014	0.24±0.04	1.50±0.21
20.478	8^+	0.11 ±0.04	0.016±0.008		0.24±0.05
20.704	8^+	$\lesssim 0.01$	~0.012	~0.073	~0.031
	(10^+)	$(\lesssim 0.12)$	(~0.085)	(~1.45)	(~0.55)

[a]Unit branching ratio assumed.
[b]$\Gamma_{\alpha 2}/\Gamma = 6 \pm 1.5\%$, taken from Ref. 42.
[c]Branching ratio taken from Ref. 17.
[d]Branching ratio taken from Ref. 41.
[e]Assumes all α_{1+2} decays go to ^{16}O(6.13;3^-).
[f]Assumes all α_{3+4} decays go to ^{16}O(6.92;2^+).

same.[28,29] The reduced widths for these particle decay channels can be obtained from our data as

$$\theta_{\lambda C}{}^2 = \Gamma_{\lambda C}\left[\frac{3}{2}\frac{\hbar^2}{\mu_c R_c{}^2}\frac{2k_c R_c}{F_l^2(k_c R_c)+G_l^2(k_c R_c)}\right]^{-1}.$$

The partial width $\Gamma_{\lambda c}$ for decay of a level λ to a channel c is obtained from measurements of the total width Γ_λ and of the branching ratio BR_c by $\Gamma_{\lambda c} = (BR_c)(\Gamma_\lambda)$. The reduced widths for decays to the excited states have been calculated assuming that the decay goes *completely* via

$$l = l_{\min} = J(^{20}\text{Ne}^*) - J(^{16}\text{O}^*)$$

and, as such, are upper limits for the reduced decay widths for that l. At the same time, because these reduced widths have been calculated for $l_{\min}$, they are also lower limits for the reduced decay widths for the state.

The value of the reduced width $\theta_{\lambda c}{}^2$ is strongly dependent on the choice of the channel radius R_c. By using the same R_c for all states decaying to that channel, however, a comparison between the relative widths should be possible. For decays to the $\alpha + {}^{16}$O channel the radius R_c was chosen to be

$$1.25(16^{1/3}+4^{1/3}) = 5.134 \text{ fm}$$

for consistency with the recent works of Sanders[5] and Young.[20] For decays to the $^{12}C + {}^8$Be channel the choice

$$R_c = 1.25(12^{1/3}+8^{1/3})$$

gave an unreasonably large reduced width for the 18.54 MeV state ($\theta_C{}^2 = 6.7$); the choice

$$R_c = 1.4(12^{1/3}+8^{1/3}) = 6.005 \text{ fm}$$

was used instead because it is the *largest* that can be reasonably justified for that channel; it gives a value of $\theta_C{}^2 = 1.50$ for the 18.54 MeV state. (Any smaller value for R_c would only increase this reduced width.) It should be emphasized that while the absolute values of these reduced widths depend sensitively on the choice of the nuclear radius, what is significant is the *comparison* of the reduced widths for any given channel evaluated using the same radius for various excited states. Such a comparison shows that the 18.54-MeV (8^+) state has a much larger reduced width for $^{12}C + {}^8$Be than any other known state in ^{20}Ne.

TABLE IV. Experimental properties of rotational bands in ^{20}Ne. Members not taken from Tables I and III are from the compilations of Ajzenberg-Selove (Ref. 7), unless otherwise noted. For the reduced width calculations, the following channel radii were used: $\theta_\alpha{}^2 \rightarrow R = 1.25(16^{1/3} + 4^{1/3}) = 5.134$ fm; $\theta_{^{12}C}{}^2 \rightarrow R = 1.4(12^{1/3} + 8^{1/3}) = 6.005$ fm.

K^π	J^π	E_x (MeV)	Γ (keV)	$\theta_{\alpha_0}{}^2$	$\theta_{\alpha_1}{}^2$	$\theta_{\alpha_2}{}^2$	$\theta_{\alpha_3}{}^2$	$\theta_{^{12}C}{}^2$
	0^+	g.s.						
	2^+	1.634	6.27×10^{-7}					
0_1^+	4^+	4.248	7.08×10^{-6}					
	6^+	8.777	0.11	0.065				
	8^+	11.949	0.035	0.0076				
	0^+	6.724	15	0.15				
	2^+	7.421	8	0.083				
0_2^+	4^+	9.999	155	0.33				
	6^+	13.927	113	0.10				
	(8^+)	20.478	250	0.11		0.016[d]		0.24
	0^+	7.191	4	0.018				
	2^+	7.829	2.4	0.010				
0_3^+	4^+	9.033	3.2	0.022				
	6^+	12.135	0.13	4.9×10^{-3}		0.66		
	8^+	15.872	100	0.047		0.94	4.2	
	0^+	8.3	>800	>0.48				
	2^+	8.8	>800	>0.91				
0_4^+	4^+	10.97	350	0.40				
	6^+	12.591	88	0.26[a]				
	8^+	17.30	213	0.20[a]				

The reduced widths extracted in this way are listed in Table III. In those cases where we could not resolve which final state the decay went to [e.g., to the 6.92 MeV (2^+) or to the 7.12-MeV (1^-) states in ^{16}O] we have calculated the reduced width assuming that the decay went to the state with the higher spin.

B. Rotational bands in ^{20}Ne

Below 10 MeV excitation in ^{20}Ne there are seven states which are believed to form the band heads for seven rotational bands, the $K^\pi = 0_1^+$, 0_2^+, 0_3^+, 0_4^+, 2^-, 0^-, and 1^- bands built on the 0_1^+ (g.s.), 0_2^+ (6.72 MeV), 0_3^+ (7.19 MeV), 0_4^+ (8.3 MeV), 2^- (4.97 MeV), 1^- (5.78 MeV), and 1^- (8.84 MeV), states, respectively. Several shell model and cluster model calculations have been performed for ^{20}Ne, and these reproduce the essential character of the different rotational bands with various degrees of accuracy. In the present work, we have been studying 8p-4h states and the degree to which they exhibit $^{12}C + {}^8Be$ clustering; one of the results of this work is the suggestion of a new 8p-4h band with good $^{12}C + {}^8Be$ cluster structure. For convenience of reference we list the experimental properties of all the known bands in ^{20}Ne in Table IV.

1. $K^\pi = 0_2^+$ band

The $K^\pi = 0_2^+$ band is thought to have predominantly the shell model configuration $(sd)^4(42)$, and therefore Fortune *et al.*[30] have suggested that the α width of the 6.72 MeV state comes from mixing with the broad ($\Gamma > 800$ keV) 0_4^+ state at 8.3 MeV which has a large α reduced width and is thought to have an $(fp)^4$ configuration.[31]

A linear extrapolation of E_x vs $J(J+1)$ for the 0^+, 2^+, and 4^+ members of the $K^\pi = 0_2^+$ band predicts the 6^+ member at 13.6 MeV and the 8^+ member at ≈ 19 MeV. The 6^+ level we observe at 13.927 MeV has an $\alpha + {}^{16}O_{g.s.}$ reduced width of 0.10, which is quite similar to the reduced widths of the other members of the $K^\pi = 0_2^+$ band; the excitation energy, the $\alpha + {}^{16}O_{g.s.}$ reduced width ($\theta_\alpha{}^2 = 0.10$), and our tentative assignment of $J^\pi = 8^+$ suggest the assignment of the state which we observe at 20.478 MeV to this band. However, for a pure $(\lambda,\mu) = (42)$ configuration, the highest L allowed is 6, and the existence of an 8^+ member would imply the admixture of higher N configurations in this

TABLE IV. (*Continued.*)

K^π	J^π	E_x (MeV)	Γ (keV)	$\theta_{\alpha_0}^2$	$\theta_{\alpha_1}^2$	$\theta_{\alpha_2}^2$	$\theta_{\alpha_3}^2$	$\theta_{^{12}C}^2$
	2^-	4.968	1.37×10^{-7}					
	3^-	5.621	3.1×10^{-6}	0.038[b]				
	4^-	7.004	1.50×10^{-6}					
2^-	5^-	8.449	0.013	0.0016				
	6^-	10.609	2.86×10^{-5}					
	7^-	13.334	0.080	2.4×10^{-4}		0.025		
	8^-							
	9^-	17.376	<10	<0.0016		<0.098		
	1^-	5.784	>0.013	>0.48				
	3^-	7.168	8	0.86				
0^-	5^-	10.261	145	0.90				
	7^-	15.336	380	0.62[a]				
	9^-	22.87	225	0.17[a]				
	1^-	8.843	19	0.011				
	3^-	10.403	81	0.048				
1^-	5^-	12.683	97	0.073				
	7^-	16.577	86	0.10				
	9^-	21.08	100	0.10[a]				
	0^+	12.436	24.4	6×10^{-4}	2.1[c]			
0_6^+								
	6^+	15.159	60	$<8\times10^{-4}$		0.05	0.91	
	8^+	18.538	138	0.0032		0.085[d]	0.24[e]	1.50

[a]Data taken from Ref. 5; see also Ref. 24 for measurements on the 17.30-MeV (8^+) level.
[b]Reference 41.
[c]Reference 35.
[d]Assumes all α_{1+2} decays go to ^{16}O*(6.13;3^-).
[e]Assumes all α_{3+4} decays go to ^{16}O*(6.92;2^+).

band. In fact, in the CCOCM calculation of Fujiwara[9] the percentages of the relative wave functions with harmonic oscillator quanta $N>10$ are 37%, 45%, 18%, and 20% for the 0^+, 2^+, 4^+, and 6^+ members, respectively. The fact that the $^{12}C + {}^8Be$ cluster channel contains the representation (42) (for $N=8$) in this model may explain why the members of this band are strongly populated at forward angles in our $^{12}C(^{12}C,\alpha)^{20}Ne$ reaction.

2. $K^\pi=0_3^+$ band

The 0^+, 2^+, 4^+, 6^+, and 8^+ members of the $K^\pi=0_3^+$ band have very small $\alpha + {}^{16}O_{g.s.}$ reduced widths[7] and very weak proton strengths,[10] while they are strongly populated in 2α transfer reactions like the $^{12}C(^{12}C,\alpha)^{20}Ne$ reaction[11–13,17] and the $^{12}C(^{14}N,{}^6Li)^{20}Ne$ reaction,[32] which led Middleton *et al.*[11] to suggest that the $K^\pi=0_3^+$ band has an 8p-4h structure. In the shell model calculation of McGrory and Wildenthal[33] the $K^\pi=0_3^+$ band is found to have a large ($>50\%$) 6p-2h component, but in the calculation of Arima and Strottman[34] the dominant component ($\approx98\%$) of the calculated 0_3^+ and 2_3^+ states is found to be 8p-4h. The only cluster calculation which reproduces the $K^\pi=0_3^+$ band is the $(^{12}C + {}^8Be) + (\alpha + {}^{16}O)$ CCOCM calculation of Fujiwara.[9]

The 10^+ member of the $K^\pi=0_3^+$ band is expected to be at ≈20.5 MeV. As demonstrated in Sec. III B 6, the spin of the 20.478 MeV state, which is strongly populated in the $^{12}C(^{12}C,\alpha)^{20}Ne$ reaction, is probably 8^+, not 10^+. (If the spin of the 20.5 MeV state were 10^+ instead of 8^+, the $\alpha + {}^{16}O_{g.s.}$ reduced width would be 1.1 which would also exclude this state from the $K^\pi=0_3^+$, 8p-4h band.) Aside from the very indeterminate situation concerning the 20.7 MeV state (Sec. III B 6) there is no evidence in our data for any states with $J^\pi=10^+$ or higher.

3. $K^\pi=0_6^+$ band

In addition to the states which fit into the $K^\pi=0_3^+$ band described above, there are a number of other ^{20}Ne excited states which have very pronounced 8p-4h character and which seem to fit together to form a $K^\pi=0_6^+$ rotational band including the 12.44-MeV (0^+), 15.16-MeV (6^+), and 18.54-MeV (8^+) states, as shown in Fig. 19. The 0^+ state at 12.44 MeV ($\Gamma=24.4\pm0.5$ keV) has branching ratios[35] of 15% for decay to the ground state of ^{16}O and 85% for decay to the 6.05-MeV (0^+) first excited state of ^{16}O which correspond to reduced widths of 6×10^{-4} ($\alpha+{}^{16}O_{g.s.}$) and 2.1 [$\alpha+{}^{16}$O (6.05 MeV; 0^+)]. The 6^+ state at 15.16 MeV (Refs. 16 and 20) has reduced widths of <0.001 ($\alpha+{}^{16}O_{g.s.}$) and 0.91 [$\alpha+{}^{16}$O (6.92 MeV; 2^+)]. The 8^+ state at 18.54 MeV has reduced widths of 0.003 ($\alpha+{}^{16}O_{g.s}$) and 1.50 (^{12}C + ^{8}Be). The ^{16}O (6.05 MeV; 0^+) and ^{16}O (6.92 MeV; 2^+) states are members of the well established[5,36] 4p-4h alpha-cluster band in ^{16}O, and hence it is clear that the primary structure of all three states is 8p-4h, ^{12}C + 2α cluster structure. The $\alpha+{}^{16}O_{g.s.}$ reduced widths of these three states are all almost one order of magnitude less than the corresponding reduced widths of members of the $K^\pi=0_3^+$ band (Table IV), indicating that admixtures of 4p configurations in these 8p-4h states are much less than that in the $K^\pi=0_3^+$, 8p-4h band. The $K^\pi=0_6^+$ band also appears to have a much more developed ^{12}C + ^{8}Be cluster structure than the $K^\pi=0_3^+$ band, as indicated by its larger moment of inertia and by the large reduced width of the 18.5-MeV (8^+) member for decay to the ^{12}C + ^{8}Be channel.

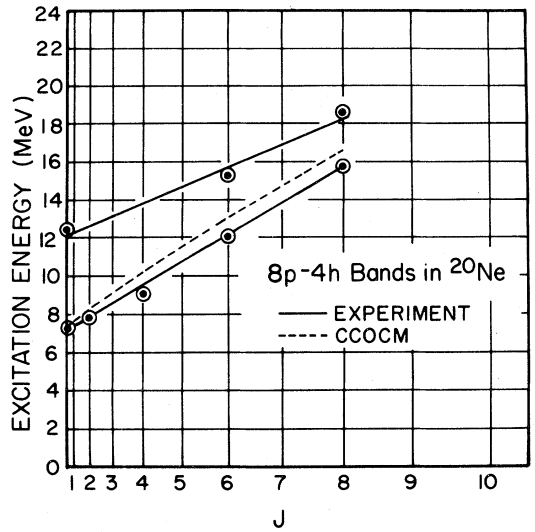

FIG. 19. Excitation energy in ^{20}Ne versus $J(J+1)$ for the $K^\pi=0_3^+$ band and other 8p-4h states. The dashed curve is the CCOCM calculation of Fujiwara (Ref. 9). The solid lines are linear fits to the experimental points.

TABLE V. Comparison of moments of inertia of selected 4p bands with 8p-4h bands and with rigid-body moments of inertia of spherical ^{20}Ne, touching spheres of $\alpha+{}^{16}$O, and touching spheres of ^{12}C + ^{8}Be. Radii of spheres taken as $R=1.4A^{1/3}$ fm.

System	$I/\hbar^2$ (MeV)$^{-1}$
^{20}Ne	2.76
$K^\pi=0_1^+$	2.94
$K^\pi=0_4^+$	4.17
$\alpha+{}^{16}$O	4.63
$K^\pi=0_3^+$	4.10
$K^\pi=0_6^+$	5.99
^{12}C + ^{8}Be	5.82

Treating the ^{8}Be cluster in the same manner as the alpha particle cluster, an analogy can be made between the 8p-4h bands ($K^\pi=0_3^+$ and $K^\pi=0_6^+$) and the two 4p bands ($K^\pi=0_1^+$ and $K^\pi=0_4^+$). In the $K^\pi=0_1^+$ band the four particles have predominantly a shell model structure as indicated by the small α reduced width and the relatively small moment of inertia; on the other hand, the particles in the $K^\pi=0_4^+$ band are better correlated and behave more like an alpha cluster on the surface of the ^{16}O core, as indicated by the large α reduced width of the $K^\pi=0_4^+$ band (Table IV) and its much larger moment of inertia relative to the ground state band (Table V). Relative to the $K^\pi=0_3^+$ band, the $K^\pi=0_6^+$ band, with its larger moment of inertia and its larger ^{12}C + ^{8}Be reduced width, could then be viewed as the 8p-4h analog of the $K^\pi=0_4^+$ band. In Table V we list the moments of inertia ($I/\hbar^2$) of these four bands, and for comparison we also show the rigid-body moments of inertia of a spherical ^{20}Ne, an $\alpha+{}^{16}$O cluster structure, and a ^{12}C + ^{8}Be cluster structure. The moments of inertia of the *cluster* bands ($K^\pi=0_4^+$ and $K^\pi=0_6^+$) are clearly larger than the corresponding *shell-model* bands ($K^\pi=0_1^+$ and $K^\pi=0_3^+$) and are surprisingly close to the simple-minded dumbbell moments of inertia.

Ikeda, Takigawa, and Horiuchi[37] proposed a model of structure change according to which the activation of the cluster degree of freedom in 4n nuclei is assumed to occur in α-cluster units with increasing excitation energy. In this model the structure of the nucleus changes from the shell structure of the ground state to a two-cluster structure and then to a multicluster structure, with such cluster structures appearing initially at or near the appropriate breakup thresholds. These results are represented schematically in the Ikeda diagram[1,37] in Fig. 20. The 12.44-MeV (0^+) state which serves

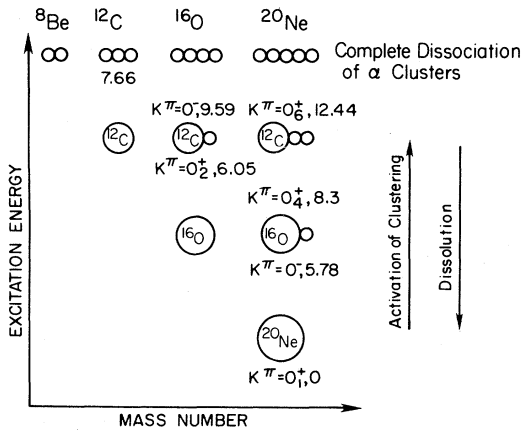

FIG. 20. Schematic representation of the structure change in light $4n$ nuclei from the shell-model-like structure of the ground state bands to the molecularlike cluster structure near thresholds for breakup to alpha particles plus residual cores. The excitation energy is in MeV. This representation is known as the Ikeda diagram and is based on figures in Refs. 1 and 37.

as the band head for the $K^\pi=0_6^+$, $^{12}C+{}^8Be$ cluster band in ^{20}Ne would correspond to the activation of the second α-cluster degree of freedom and is quite consistent with this model, occurring very close to the 11.98-MeV threshold for breakup into $^{12}C+{}^8Be$. The large reduced width of the 18.5-MeV state for decay to $^{12}C+{}^8Be$ suggests that the two α particles outside the ^{12}C core are correlated, and hence our direct observation of the *correlated* 2-α decay of the 18.5-MeV state goes one step further in determining the nature of clustering in the $^{12}C+2\alpha$ structure of the $K^\pi=0_6^+$ band and suggests the occurrence in ^{20}Ne of a large-scale molecular-type structure which may provide a connection between simple alpha clustering and quasimolecular resonances.

To establish the $K^\pi=0_6^+$ band and its cluster properties on a firmer basis appropriate 2^+ and 4^+ members will have to be found. Groups at the University of Washington[38] and the University of Wisconsin[39] are currently studying $^{16}O(\alpha,\alpha)$ elastic and inelastic scattering in the region $E_x=12.5-14.5$ MeV in order to search for $J^\pi=2^+$ and 4^+ resonances with large reduced widths for α decay to the 4p-4h states at 6.05 MeV (0^+) and 6.92 MeV (2^+) in ^{16}O.

V. SUMMARY AND CONCLUSIONS

With the aim of studying the cluster structure of 8p-4h states in ^{20}Ne, we have measured the spins, widths, and decay properties of several states populated in the $^{12}C(^{12}C,\alpha)^{20}Ne$ reaction at $E(^{12}C)=64$ and 80 MeV. In addition to confirming the spins of several lower-lying states, we have assigned a spin of 8^+ to the state at 18.538 MeV and have suggested spins for the states at 17.259 MeV (7^-), 20.478 MeV (8^+), and 24.374 (7^-). We have assigned the 13.927-MeV (6^+) state to the $K^\pi=0_2^+$ band, and suggested the extension of this band to the 8^+ level at 20.478 MeV. We have assigned the 16.600-MeV (7^-) level to the $K^\pi=1^-$ band. The strong population of the $K^\pi=0_2^+$, 1^-, and 2^- bands in our $^{12}C(^{12}C,\alpha)^{20}Ne$ spectra at bombarding energies 60 MeV $<E(^{12}C)\leq 80$ MeV as well as in other 8 particle transfer reactions, such as $^{12}C(^{16}O,{}^8Be)^{20}Ne$ and $^{12}C(^{14}N,{}^6Li)^{20}Ne$, may be partially explained by the fact that the dominant SU(3) configuration of these bands is contained in the SU(3) classification of the allowed $^{12}C+{}^8Be$ cluster wave function.

The 18.538 MeV (8^+) state was found to have a large reduced width for decay into the $^{12}C+{}^8Be$ channel, which, together with a small reduced width for decay into $\alpha+{}^{16}O_{g.s.}$, suggests that this state has a large component of $^{12}C+{}^8Be$ cluster structure. We have suggested the assignment of this state to a new 8p-4h band which has the 12.436-MeV (0_6^+) state as its band head and which includes the state at 15.159 MeV as its 6^+ member. The moment of inertia of this 8p-4h band is larger than that of the $K^\pi=0_3^+$ 8p-4h band and is approximately equal to the classical moment of inertia of two touching spheres with the masses and radii of ^{12}C and ^{8}Be.

The evolution of 8p-4h structure with increasing excitation energy, from the shell-model-like structure of the $K^\pi=0_3^+$ band to the $^{12}C+{}^8Be$ cluster structure of the $K^\pi=0_6^+$ band, is similar to the evolution of 4p structure from the shell-model structure of the ground state ($K^\pi=0_1^+$) band to the $\alpha+{}^{16}O_{g.s.}$ cluster structure of the $K^\pi=0^-$ and 0_4^+ bands. The proposed $K^\pi=0_6^+$ band should serve as a link between the α cluster bands in light nuclei (^{8}Be, ^{12}C, ^{16}O, ^{20}Ne), and the ^{12}C-^{12}C quasimolecular bands in ^{24}Mg.[40]

This research was supported by the U.S. Department of Energy under Contract No. DE-AC02-76ER03074.

*Present address: Physics Department, University of Petroleum and Minerals, Dhahran, Saudi Arabia.

†Present address: Physics Division-203, Argonne National Laboratory, Argonne, IL 60439.

[1]For example, H. Horiuchi, in *Proceedings of the International Conference on Nuclear Structure, Tokyo, 1977,* edited by T. Marimori (Physical Society of Japan, Tokyo, 1978) Suppl. [J. Phys. Soc. Jpn. 44, 85 (1978)], and references therein; H. Horiuchi, in *Clustering Aspects of Nuclear Structure and Nuclear Reactions (Winnipeg, 1978),* Proceedings of the Third International Conference on Clustering Aspects of Nuclear Structure and Nuclear Reactions, AIP Conf. Proc. No. 47, edited by W. T. H. Van Oers, J. P. Svenne, J. S. C. McKee, and W. R. Falk (AIP, New York, 1978).

[2]E. C. Halbert, J. B. McGrory, B. H. Wildenthal, and S. Panda, Adv. Nucl. Phys. 4, 315 (1971); J. B. McGrory and B. H. Wildenthal, Phys. Rev. C 7, 974 (1973).

[3]H. C. Lee and R. Y. Cusson, Phys. Rev. Lett. 29, 1525 (1972); G. Ripka, Adv. Nucl. Phys. 1, 183 (1968).

[4]M. E. Cobern, D. J. Pisano, and P. D. Parker, Phys. Rev. C 14, 491 (1976); J. D. MacArthur, H. C. Evans, J. R. Leslie, and H. B. Mak, *ibid.* 22, 356 (1980).

[5]S. J. Sanders, L. M. Martz, and P. D. Parker, Phys. Rev. C 20, 1743 (1979).

[6]T. Matsuse, M. Kamimura, and Y. Fukushima, Prog. Theor. Phys. 53, 706 (1975).

[7]F. Ajzenberg-Selove, Nucl. Phys. A300, 1 (1978); A392, 1 (1983).

[8]F. Nemoto, Y. Yamamoto, H. Horiuchi, Y. Suzuki, and K. Ikeda, Prog. Theor. Phys. 54, 104 (1975); T. Tomoda and A. Arima, Nucl. Phys. A303, 217 (1978).

[9]Y. Fujiwara, H. Horiuchi, and R. Tamagaki, Prog. Theor. Phys. 61, 1629 (1979); Y. Fujiwara, *ibid.* 62, 122 (1979); 62, 138 (1979).

[10]R. R. Betts, H. T. Fortune, and R. Middleton, Phys. Rev. C 11, 19 (1975).

[11]R. Middleton, J. D. Garret, and H. T. Fortune, Phys. Rev. Lett. 27, 950 (1971).

[12]A. D. Panagioutou, H. E. Gove, and S. Harar, Phys. Rev. C 5, 1995 (1972).

[13]L. R. Greenwood, R. E. Segel, K. Raghunathan, M. A. Lee, H. T. Fortune, and J. R. Erskine, Phys. Rev. C 12, 156 (1975).

[14]M. M. Hindi, Ph.D. thesis, Yale University, 1980 (unpublished).

[15]A. E. Litherland and A. J. Ferguson, Can. J. Phys. 39, 788 (1961).

[16]L. K. Fifield, R. W. Zurmühle, D. P. Balamuth, and J. W. Noé, Phys. Rev. C 8, 2203 (1973).

[17]K. C. Young, Jr., Ph.D. thesis, University of Pennsylvania, 1978 (unpublished).

[18]M. M. Hindi, J. H. Thomas, D. C. Radford, and P. D. Parker, Phys. Lett. 99B, 33 (1981).

[19]H. J. Rose and D. M. Brink, Rev. Mod. Phys. 39, 306 (1967).

[20]K. C. Young, Jr., R. W. Zurmühle, J. M. Lind, and D. P. Balamuth, Nucl. Phys. A330, 452 (1979).

[21]M. K. Mehta, W. E. Hunt, and R. H. Davis, Phys. Rev. 160, 791 (1967).

[22]K. P. Artemov, V. Z. Gol'dberg, I. P. Petrov, V. P. Rudakov, I. N. Serikov, and V. A. Timofeev, Yad. Fiz. 21, 1157 (1975) [Sov. J. Nucl. Phys. 21, 596 (1976)].

[23]L. R. Medsker, H. T. Fortune, R. R. Betts, and R. Middleton, Phys. Rev. C 11, 1880 (1975).

[24]J. H. Billen, Phys. Rev. C 20, 1648 (1979); Bull. Am. Phys. Soc. 22, 527 (1977).

[25]O. Häusser, T. K. Alexander, D. L. Disdier, A. J. Ferguson, A. B. McDonald, and I. S. Towner, Nucl. Phys. A216, 617 (1973).

[26]C. M. Fou, D. P. Balamuth, R. W. Zurmühle, and K. C. Young, Jr., Phys. Rev. C 20, 1754 (1979).

[27]C. Bergman and R. K. Hobbie, Phys. Rev. C 3, 1729 (1971).

[28]A. Arima and S. Yoshida, Phys. Lett. 40B, 15 (1972); A. Arima, H. Horiuchi, K. Kudobera, and N. Takigawa, Adv. Nucl. Phys. 5, 345 (1972).

[29]M. Ichimura, A. Arima, E. C. Halbert, and T. Terasawa, Nucl. Phys. A204, 255 (1973).

[30]H. T. Fortune, R. Middleton, and R. R. Betts, Phys. Rev. Lett. 29, 738 (1972).

[31]D. Strottman, N. Anyass-Weiss, J. C. Cornell, P. S. Fisher, P. N. Hudson, A. Menchaca-Rocha, A. D. Panagioutou, and D. K. Scott, Phys. Lett. 47B, 16 (1973).

[32]K. Nagatani, M. J. Levine, T. A. Belote, and A. Arima, Phys. Rev. Lett. 27, 1071 (1971).

[33]J. B. McGrory and B. H. Wildenthal, Phys. Rev. C 7, 974 (1973).

[34]A. Arima and D. Strottman, Nucl. Phys. A162, 423 (1971).

[35]E. F. Garman, L. K. Fifield, W. N. Catford, D. P. Balamuth, J. M. Lind, and R. W. Zurmühle, Nucl. Phys. A372, 194 (1981).

[36]Y. Suzuki, Prog. Theor. Phys. 55, 1751 (1976); 56, 111 (1976).

[37]K. Ikeda, N. Takigawa, and H. Horiuchi, Prog. Theor. Phys. Suppl. Extra Number (1968), p. 464.

[38]M. M. Hindi, D. H. Dowell, K. A. Snover, private communication.

[39]G. Caskey, private communication.

[40]For example, K. A. Erb, D. A. Bromley, J. Weneser, Comments Nucl. Part. Phys. 8, 111 (1978).

[41]O. Häusser, A. J. Ferguson, A. B. McDonald, I. M. Szöghy, T. K. Alexander, and D. L. Disdier, Nucl. Phys. A179, 465 (1972).

[42]D. P. Balamuth, J. W. Nóe, H. T. Fortune, and R. W. Zurmühle, Phys. Rev. C 6, 1964 (1972).